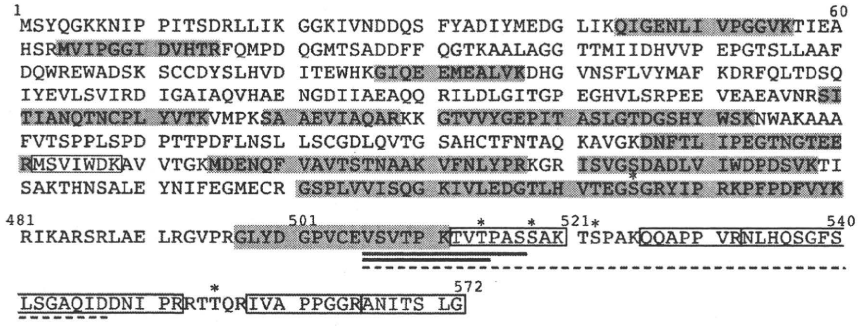

Figure 3 Summary of the LC/MS analysis. Gray: detected in the tryptic digests of both spots *a* and *b1*; white box: detected in the tryptic digest of spot *b1*; red underline: detected in the Glu-C digest of spot *a* ($[M+H]^+$ = 1186.8); blue underline: detected in the Glu-C digest of spot *a* ($[M+H]^+$ = 913.7); broken underline: expected to be obtained by the Glu-C digestion of full-length CRMP-2; *: the potential phosphorylation sites. The sequence is from UniProtKB; O08553.

result, the amounts of CRMP-2-ΔC became comparable to those observed for the full-length form of CRMP-2 (Figure 4B, left). This change of CRMP-2-ΔC in the late stages of the disease was further confirmed by the examination of an additional number of specimens (Additional file 1). This modest but statistically significant change appeared to account for the focal distribution of lesions in the brain [1-3].

Analysis of the CRMP-2 transcript

Two variant forms of CRMP-2, named CRMP-2A and -2B, were previously identified that had different amino terminal regions due to the alternative usage of two first coding exons [30-33]. Therefore, we examined if the occurrence of CRMP-2-ΔC was due to alternative splicing or post-translational processing. Using Northern blot analysis, a single 4.5-kb band was invariably detected in the prion-infected mice (n = 2) and the mock controls (n = 2) sacrificed at 160 dai (Figure 4C). This size was substantially the same as for the previously reported CRMP-2 gene transcript [17,19]; accordingly, we conceived that CRMP-2-ΔC was not produced by alternative splicing, but by post-translational proteolytic cleavage. It should be noted that densitometric analysis of the bands did not show significant difference in the mRNA levels of CRMP-2 between the prion-infected and the control mice after normalization to the amount of glyceraldehyde-3-phosphate dehydrogenase (GAPDH) mRNA (Figure 4C, right). In a further analysis by quantitative RT-PCR to compare the mRNA levels of CRMP-2 in the two groups of mice in detail, we again did not find a statistical difference in the level of CRMP-2 mRNA between the prion-infected mice and the mock controls (Additional file 2).

Effects of the overexpression of CRMP-2-ΔC on neurons *in vitro*

Considering the increasing ratio of CRMP-2-ΔC to full-length CRMP-2 in the late stages of prion disease in our model (Figure 4), we asked whether CRMP-2-ΔC would affect the morphology of the neurites. Plasmids encoding full-length CRMP-2 (named CRMP-2-wt), CRMP-2-ΔC, or phosphorylated or non-phosphorylated mimics named CRMP-2/DD, /AD, /DA, and /AA, in which the C-terminal potential phosphorylation sites Thr^{514} and Thr^{555} [20] were mutagenized to Asp or Ala (Figure 5A), were introduced into murine embryonic cerebral neurons on the first day of culture *in vitro* (0-DIV). As the transfection efficacy of the neurons in primary culture was rather low, we co-transfected a plasmid encoding green fluorescent protein (GFP) to identify the transfected cells. The cells positive for GFP-fluorescence were examined at 4-DIV for neurites longer than 10 μm, and we found that the cells transfected with CRMP-2-ΔC developed 1.2-fold more neurite tips than the cells transfected with the empty vector (Figures 5B and 5C). An enhanced level of branching of the neurite tips was also observed in the cells expressing the non-phosphorylated mimic CRMP-2/AA (Figures 5B and 5C). Conversely, the cells transfected with CRMP-2-wt exhibited slightly fewer neurite branch tips than the cells transfected with the empty vector, similar to the cells transfected with CRMP-2/DD (Figures 5B and 5C). This was presumably because cellular kinases phosphorylated CRMP-2-wt that, in turn, acted against the development of neurite tips. In contrast to the range of variation in branching, the length of the longest neurites did not show a significant difference and were in the range of 269.8 ± 10.1 μm (Figure 5D).

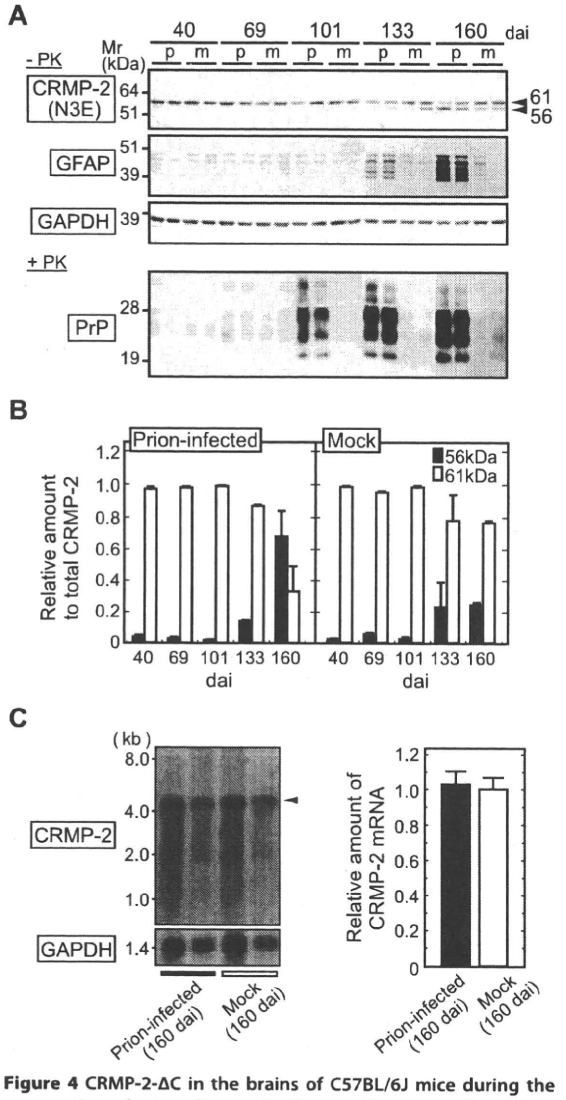

Figure 4 CRMP-2-ΔC in the brains of C57BL/6J mice during the progression of prion disease. (A) Western blot analysis for CRMP-2, GFAP and GAPDH. The accumulation of PK-resistant PrP^{Sc} is shown at the bottom. p: prion-infected; m: mock controls. The ladders of GFAP bands are possibly due to post-translational cleavage [24] or alternative splicing [51]. (B) The amounts of 61-kDa and 56-kDa CRMP-2 relative to the total amount of CRMP-2 as determined from the signal intensity of the bands in panel (A). Data are means ± SEM (n = 2). (C) Northern blot analysis for prion-infected and mock-infected mice sacrificed at 160 dai (n = 2, respectively). The arrowhead indicates the CRMP-2 transcript. The ratios of signal intensities of the bands of CRMP-2 mRNA to that of GAPDH mRNA are shown after normalization to the ratio obtained from the control mice as 1.00 (means ± SEM).

Discussion

CRMPs are cytosolic phosphoproteins abundantly expressed in the developing brain [16-20,31], and in some neurons and oligodendrocytes in the adult brain [17,19,32,33]. Among the five known isoforms (CRMP-1 to -5), CRMP-2 was originally identified as a mediator of the collapse of growth cones by semaphorin [16], and later shown to be involved in the outgrowth of axons and the induction of neuronal polarity [20] in developing neurons. Further studies also showed different splicing patterns of its mRNA, giving rise to two variant forms named CRMP-2A and -2B [30]. CRMP-2A (theoretical Mr of 75 kDa) has a long N-terminal sequence, and induces oriented microtubule patterns in cultured fibroblasts [30]. On the other hand, the shorter variant CRMP-2B (theoretical Mr of 62 kDa) corresponds to the originally identified CRMP-2 protein, and favors disoriented microtubule patterns in the fibroblasts [30]. Thus, the two variants seem to display different, or even opposite functional properties [30,32]. Intriguingly, Western blot analysis of the brain of mouse [32] and rat [33] showed that CRMP-2A is mainly expressed in the developing brain while CRMP-2B is predominantly expressed in the adult brain. The temporal expression pattern of the two forms, together with their distinct functions, suggest that CRMP-2 plays roles more than the axonal outgrowth and the induction of neuronal polarity.

Not only in the physiological neuronal processes, the importance of CRMP-2 in the adult brain under non-physiological conditions has also been implied recently in animal models of neurodegenerative disorders including traumatic brain injury and cerebral ischemia (see below). Here, we performed a proteomic analysis of the brains of mice infected with scrapie prion, and found a C-terminally truncated form of CRMP-2 (CRMP-2-ΔC) in the late pathological stages of the disease. To date, truncated forms of CRMP-2 have been identified in cultured neurons exposed to N-methyl-D-aspartic acid [34,35] or depleted of nerve growth factor [36], in models of traumatic brain injury [35,37], ischemia [38], and sciatic nerve injury [39], and in the developing mouse brain [31]. Although the precise cleavage sites of CRMP-2 in these studies remain undetermined, sequence-specific antibodies [34,35] or peptide mapping in MS analyses [31,36,39] mapped them to the C-terminal region. In addition, some studies ascribed proteolytic cleavage by calpain to the production of the truncated forms of CRMP-2 [34-36]. We demonstrated that the production of CRMP-2-ΔC was not due to the alternative splicing of its mRNA, the known splicing responsible for the production of CRMP-2A and -2B [30]. Rather, judging from its Mr_{obs}, pI_{obs} and the truncation site, it is most conceivable that CRMP-2-ΔC was derived from proteolytic cleavage of CRMP-2B (referred to as the full-length form of CRMP-2 in the present study) which is predominantly expressed in the adult brain [32,33]. We speculate that calpain is likely to be involved in its generation, since the truncation site of

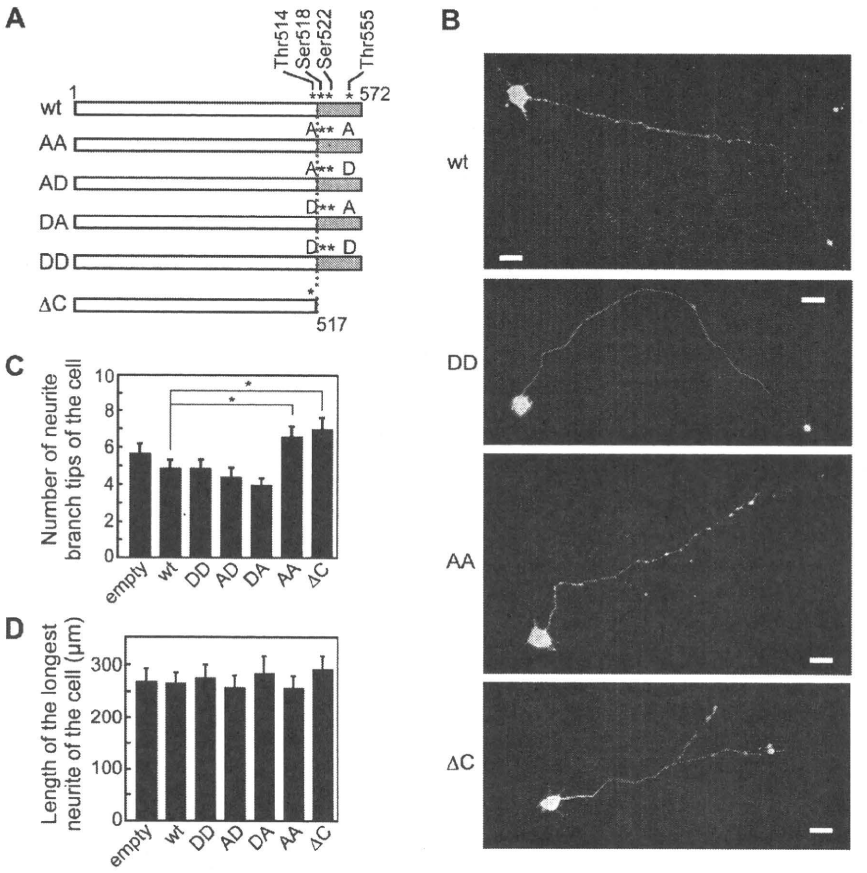

Figure 5 Effect of CRMP-2-ΔC on primary cultured neurons. (A) Diagram of the cDNA constructs. The asterisks show the potential phosphorylation sites in the C-terminal region. (B) Representative images of the neurons at 4-DIV. Bar; 20 μm. (C) Numbers of neurite branch tips longer than 10 μm in individual cells at 4-DIV. Data are means ± SEM from at least 24 cells. *Statistical difference determined by Student's t-test (*P*0.05). (D) Lengths of the longest neurites of the cells at 4-DIV. Data are means ± SEM of the lengths from at least 24 cells.

CRMP-2-ΔC (P_4 = Thr, P_3 = Pro, P_1' = Ser, and P_2' = Ala) was in modest agreement with the amino acid sequences preferred for cleavage by calpain [40,41]. In this regard, an increased level of μ-calpain was reported in the hippocampus of prion-infected mice [24]. It should be noted that a recent quantitative RT-PCR analysis of the brains of C57BL/6 mice challenged with bovine spongiform encephalopathy prion showed an increased level of CRMP-2 mRNA approximately to 140% of that in the control mice in the mid-stage of the disease, and its decrease to 54% in the terminal stage [42]. We have shown the level of CRMP-2 mRNA did not differ significantly between the prion-infected and the control mice in the late phase of the disease (Figure 4C, Additional file 2). The reason for this discrepancy in the decreased level of CRMP-2 mRNA in the later stages of the disease remains unknown at the moment. It might be due to the difference in the prion strains, or the difference in the pathological severity at the timing of the specimen sampling. The truncation of CRMP-2 was not mentioned in this transcriptional study [42].

Lines of evidence to date indicate that the sequential phosphorylation of CRMP-2 at Ser^{522}, Thr^{509}, Thr^{514} and Ser^{518} by Cdk5 and GSK-3β is essential for the regulation of CRMP-2 activity [20,29]. These regulatory sites are, however, partially ablated in CRMP-2-ΔC. In fact, the unchanged pI value of CRMP-2-ΔC after incubation with λ-PPase (Figure 1E), and the absence of a neutral loss of H_3PO_4 ($\Delta m/z$ = -98) in the MS analysis of CRMP-2-ΔC (data not shown), strongly indicated that it was not phosphorylated. Thus, the augmentation in the development of neurite branch tips of cultured neurons by the overexpression of CRMP-2-ΔC may be explained by the lack of the regulatory phosphorylation sites. Alternatively, it is recognized that CRMPs are assembled into homo- or hetero-tetramers. Interestingly, while the structure of the recombinant $CRMP\text{-}2^{13\text{-}490}$ (i.e., lacking the C-terminal region) was indeed in a

tetrameric form, as determined using crystallographic analysis, it behaved like a trimer when analyzed using gel filtration [43]. This was interpreted to indicate a rapid equilibrium between the tetrameric and the dimeric states of CRMP-2^{13-490} [43]. If so, it is conceivable that CRMP-2-ΔC has a reduced ability to undergo oligomerization. Such a defect in oligomerization into the homomeric and/or heteromeric state would impair the physiological function of CRMP-2. In the adult brain, CRMP-2B is the predominant form of CRMP-2, and mainly localizes in dendrites [32]. Considering that hamster [2] and murine [3] models of scrapie showed neuronal dendritic atrophy before ultimate neuronal cell death, it is interesting to surmise that CRMP-2-ΔC might be involved in such a neurodegenerative process.

Conclusions

To explore the molecular neuropathology of prion diseases, we conducted a proteomic analysis of a murine model of prion diseases. In addition to the quantitative changes of GFAP, glutathione S-transferase-μ1 and peroxiredoxins during the progression of the disease in the brain of ICR and C57BL/6J mice, we identified a unique truncation of CRMP-2. Detailing the relevance of CRMP-2-ΔC to the morphological abnormalities of degenerating axon terminals/dendrites observed in models of scrapie [1-3] awaits further study. Nevertheless, considering that several forms of truncated CRMP-2, if not identical to CRMP-2-ΔC, were found in models of neurodegenerative disorders [35-39], the results of the present study should provide clues to the molecular neuropathology of prion diseases compared with other neurodegenerative disorders.

Methods

Mice, prion inoculation, and brain homogenate

Female C57BL/6J and ICR mice (6 weeks old) were purchased from Charles River Laboratories (Yokohama, Japan) and CLEA Inc. (Meguro, Japan), respectively. The mice were inoculated with 25 μL of a 0.25% (w/v) brain homogenate in phosphate-buffered saline (PBS; JRH Biosciences, Lenexa, USA) prepared from terminally ill ICR mice infected with mouse-adapted scrapie prion (Obihiro-I strain) [21]. As mock-infected controls, mice were injected with 25 μL of a 0.25% brain homogenate (w/v in PBS) from healthy mice. Experiments were carried out in compliance with the biosafety regulations and the guidelines for laboratory animal care of the National Institute of Infectious Diseases. Individual brains were homogenized in 4-volumes (w/v) of chilled PBS using a Physcotron homogenizer (Microtec Co., Ltd., Funabashi, Japan), and centrifuged at 100,000 × *g* for 1 h at 4°C with a TLA-55 rotor (Beckman Coulter, Inc., Fullerton, USA) to obtain the supernatant (soluble fraction) and the pellet (membranous fraction). Protein concentrations were determined using a BCA protein assay kit (Pierce, Rockford, USA).

2-DE

The samples were prepared by adjusting the soluble fraction of the brain homogenate to a total of 400 μg protein/mL in 9 M Urea, 4% CHAPS, 65 mM DTT, and 0.5% IPG buffer 3-10 (GE Healthcare, Uppsala, Sweden). Immobiline DryStrips for isoelectric focusing (IEF; pH 3-10 NL, 13 cm, GE Healthcare) were rehydrated at 20°C overnight by soaking in 250 μL of the sample solution (a total of 100 μg of protein), then IEF was carried out using a linear gradient from 0-1000 V in 2 h, followed by 8000 V for 6 h. After IEF, the strips were equilibrated with 50 mM Tris-HCl (pH 8.8), 6 M urea, 2% SDS, 20 mM DTT, 30% glycerol, and 0.03% bromophenol blue for 15 min, and overlaid on 12.5% polyacrylamide slab gels for SDS-PAGE. Proteins were stained with CBB R-250 or SYPRO Ruby (Invitrogen, Carlsbad, USA), and gel images were captured using a LAS-1000 plus lumino-image analyzer (Fuji Photo Film, Tokyo, Japan). Software PDQuest, version 7.3 (Bio-Rad Laboratories, Hercules, USA) was used for the image analysis. At least one duplicate set of mice was analyzed for each specified dai. Mr and pI were calibrated using the spots of the following proteins: calmodulin (16.7 κDa, pI 4.1), γ-enolase (47.2, 5.0), serum albumin (65.9, 5.5), peroxiredoxin 6 (24.7, 5.72), carbonic anhydorase II (28.9, 6.5), and aconitase (82.5, 7.4). The signal intensity of each spot was normalized to that of β-actin for statistical analysis. In the dephosphorylation analysis, the samples were incubated with λ-PPase (New England Biolabs, Inc., Beverly, USA) at 30°C for 15 min prior to 2-DE.

Western blotting

The anti-CRMP-2 antibodies C4G (epitope; CRMP-$2^{480-528}$) and N3E (epitope; CRMP-$2^{142-194}$) [29] were purchased from Immuno-Biological Laboratories Co., Ltd. (Takasaki, Japan). The other antibodies used were anti-GFAP (DAKO, Glostrup, Denmark), anti-GAPDH from (Abcam plc., Cambridge, UK), HRP-labeled anti-mouse IgG (TrueBlot) (eBioscience Inc., San Diego, USA), and HRP-labeled anti-rabbit IgG F(ab')$_2$ (GE Healthcare). The ECL Plus reagent (GE Healthcare) and a LAS-3000mini lumino-image analyzer (Fuji Photo Film) were used for detection. Signal intensity was quantified using Image Gauge software (Fuji Photo Film). For the analysis of PrP^{Sc}, the membranous fraction (a total of 10 μg proteins) in 30 μL of 0.5% sarkosyl, 25 mM Tris-HCl, and 50 mM NaCl (pH 7.5) was incubated with PK (final concentration, 0.1 μg/μL) at 37°C for 120 min. The digestion was stopped by the addition of 4-volumes of 10 mM phenylmethylsulfonyl fluoride in methanol, and the mixture

was centrifuged at 20,000 × *g* for 30 min at 4°C to recover PrP^{Sc} as a precipitate. The anti-PrP monoclonal antibody 44B-1 [44] was a gift from Prof. M. Horiuchi (Hokkaido University, Japan).

MS and protein identification

Pieces of the 2-DE gel were rinsed with 100 mM ammonium bicarbonate, and incubated with 10 mM DTT at 56°C for 45 min. Then, protein in the gel was reacted with 55 mM iodoacetamide at room temperature for 45 min, and subjected to in-gel digestion [45,46] with trypsin (sequencing grade; Promega, Madison, USA) or Glu-C (EC 3.4.21.19; Roche Applied Science, Basel, Switzerland). For the peptide-mass fingerprint analysis, MS data for the tryptic digests obtained with a Voyager-DE STR spectrometer (Applied Biosystems, Foster City, USA) were examined in the NCBInr.fasta protein database using MS-Fit [47] and Mascot/version 2.1 (Matrix Science, Boston, USA) software [48]. For the amino acid sequence analysis of CRMP-2, the digests were applied to a MAGIC2002 HPLC system (Michrom Bioresources, Inc., Auburn, USA) equipped with a capillary column (Inertsil ODS 3 μm, 0.1 mm i.d. × 50 mm, GL Science Inc., Shinjuku, Japan). Elution was performed using (A) H_2O/acetonitrile/formic acid = 98/2/0.1 (v/v/v) and (B) H_2O/acetonitrile/formic acid = 10/90/0.1 (v/v/v), with a gradient from A/B = 95/5 (v/v) to 45/55 (v/v) at a flow rate of 400 nL/min. The eluate was introduced into an LCQ Deca XP spectrometer (Thermo Fisher Scientific Inc., Waltham, USA) using a nano-ESI interface (AMR Inc., Meguro, Japan) and a MonoSpray FS monolithic emitter (GL Sciences). The data were collected at an interval of three tandem spectra per spectrum in the data-dependent-scan mode, and analyzed using BioWorks software (Thermo Fisher Scientific Inc., version 3.1) and by manual inspection. The theoretical Mr and pI values were calculated using Compute pI/MW [49] and Scansite [50] software.

Northern blotting

RNA was prepared from the whole brains of C57BL/6J mice sacrificed at 160 dai using the SV Total RNA Isolation System (Promega), and stored at -80°C in RNA*secure*reagent (Applied Biosystems) until use. Electrophoresis was carried out with 1 μg of RNA using 1.0% agarose-formaldehyde gel in 40 mM MOPS-NaOH, 10 mM sodium acetate, and 1 mM EDTA (pH 7.0). After the transfer of the RNA to a positively charged-nylon membrane (Roche Applied Science), the membrane was incubated with digoxigenin-labeled antisense RNA probes for CRMP-2 (complementary to the open reading frame (ORF) from +340 to +1551; corresponding to Thr^{114}-Ser^{517}) or GAPDH (the ORF of from +330 to +878) at 68°C overnight in Ambion ULTRAhyb hybridization buffer (Applied Biosystems). The bound probes were detected using an alkaline phosphatase-labeled anti-digoxigenin antibody (Roche Applied Science) and CDP-Star chemiluminescence reagent (New England Biolabs, Inc.), with X-ray films (Fuji Photo Film) and a LAS-3000mini lumino-image analyzer (Fuji Photo Film). Signal intensity was quantified using Image Gauge software (Fuji Photo Film).

Plasmids

Full-length cDNA of mouse CRMP-2-wt was obtained from a C57BL/6J mouse brain cDNA library (Invitrogen) by PCR using the following primers: 5'- GGAATTCGAGATGTCTTATCAGGGGAAGAAAAATATTCCA-3' and 5'- ATAAGAATGCGGCCGCTTTAGCCCAGGCTGGTGATGTTGG-3' (the underlined sequences are for the generation of *Eco*RI and *Not*I sites). CRMP-2-ΔC cDNA ($CRMP\text{-}2^{1\text{-}517}$) was generated using the reverse primer 5'- ATAAGA ATGCGGCCGCTTATGAGGCTGGAGTCACC-3' (the underlined sequence is for the introduction of a *Not*I site). The cDNAs were ligated into the pCIneo mammalian expression vector (Promega) between the *Eco*RI and *Not*I sites. Site-directed mutagenesis was carried out using the following primers: 5'- GTGACGCCCAAGACGGTGGCGCCAGCCTCATCAGCTAAG-3' and 5'- CTTAGCTGATGAGGCTGGCGCCACCGTCTTGGGCGTCAC-3' for T514A; 5'-GTGACGCCCAAGACGGTGGATCCAGCCTCATCAGCTAAG-3' and 5'- CTTAGCTGATGAGGCTGGATCCACCGTCTTGGGCGTCAC-3' for T514D; 5'-CATTCCCCGCCGCACCGCCCAGCGCATCGTGG-3' and 5'- CCACGATGCGCTGGGCGGTGCGGCGGGGAATG-3' for T555A; and 5'- CATTCCCCGCCGCACTGATCAGCGCATCGTGG-3' and 5'- CCACGATGCGCTGATCAGTGCGGCGGGGAATG-3' for T555D. The constructs were verified using DNA sequencing.

Cell culture, transfection, and microscopy

Cerebral cortical neurons from E15 ICR mice (Nerve-cell Culture System; Sumitomo Bakelite Co., Ltd., Shinagawa, Japan) were plated on poly-L-lysine-coated plastic dishes (Sumitomo Bakelite Co., Ltd.), and maintained in Neurobasal medium (Invitrogen-GIBCO) with B27 (Invitrogen-GIBCO) and 0.5 mM glutamine according to the manufacturer's instructions. Arabinocytidine (2.5 μM) was added to the medium to suppress the growth of glia. The pCIneo vectors encoding CRMP-2 or its mutants (1 μg) were mixed with pEGFP-N1 encoding GFP (0.5 μg; Clontech Laboratories Inc., Mountain View, USA), and the mixture was introduced into cells using the NeuroPORTER transfection reagent (Genlantis, San Diego, USA) at the time of plating (0-DIV). The neurons were fixed at 4-DIV using BD Cytofix (BD

Biosciences, Franklin Lakes, USA) for 15 min at room temperature, and observed under a BIOZERO BZ-8000 microscope (Keyence, Osaka, Japan) with a software BZ analyzer (Keyence) for counting the number of neurite tips and measuring the length of neurites.

Additional material

Additional file 1: CRMP-2-ΔC in the brains of C57BL/6J mice in the late stages of the disease. A supplementary data of Western blot analysis for detection of CRMP-2-ΔC in additional individuals of prion-infected and mock control mice.

Additional file 2: Relative levels of CRMP-2 mRNA determined by quantitative RT-PCR. The mRNA levels of CRMP-2 did not show significant difference between the prion-infected and mock control mice in quantitative RT-PCR analysis.

List of abbreviations

CRMP-2: collapsin response mediator protein-2; **2-DE**: two-dimensional electrophoresis; **dai**: days after inoculation; **DIV**: day of culture *in vitro*; **GAPDH**: glyceraldehyde-3-phosphate dehydrogenase; **GFAP**: glial fibrillary acidic protein; **GFP**: green fluorescent protein; **Glu-C**: endoproteinase Glu-C; **IEF:** isoelectric focusing; **λ-PPase**: lambda phosphatase; **LC-ESI-MS/MS**: liquid chromatography-electrospray ionization-tandem mass spectrometry; **MALDI**: matrix-assisted laser desorption/ionization; **Mr**: molecular mass; $\mathbf{Mr_{obs}}$: observed Mr; **MS**: mass spectrometry; **ORF**: open reading frame; **PBS:** phosphate-buffered saline; $\mathbf{pI_{obs}}$: observed pI; PK: proteinase K; **PrP**: prion protein; $\mathbf{PrP^{C}}$: cellular prion protein; $\mathbf{PrP^{Sc}}$: disease-associated prion protein

Competing interests

The authors declare that they have no competing interests.

Authors' contributions

FSO performed the experiments, data analysis and protein identification, and wrote the manuscript. **YY** took care of the mice, collected tissue samples, provided experimental devices, and took part in the experimental design. **HH** took care of the mice and collected tissue samples. **MT** helped perform the cell culture experiments. **MN** and **KH** took part in the experimental design. **KH** performed a Northern blotting analysis, participated in the experimental design, data analysis, and wrote the manuscript. All authors read and approved the final manuscript.

Acknowledgements

We thank Prof. M. Horiuchi (University of Hokkaido) for the anti-PrP antibody 44B1. This work was supported by Grants-in-aid for BSE Research from MHLW, Japan (20330701, YY and KH) and for Exploratory Research from MEXT, Japan (17659024, KH).

Author details

[1]Department of Biochemistry and Cell Biology, National Institute of Infectious Diseases, 1-23-1, Toyama, Shinjuku-ku, Tokyo 162-8640, Japan. [2]Department of Pathology, National Institute of Infectious Diseases, 1-23-1, Toyama, Shinjuku-ku, Tokyo 162-8640, Japan. [3]National Institute of Health Sciences, Kamiyoga, Setagaya-ku, Tokyo 158-8501, Japan.

Received: 11 June 2010 Accepted: 20 October 2010
Published: 20 October 2010

References

1. Prusiner SB, (Ed): *Prion biology and diseases* Cold Spring Harbor: Cold Spring Harbor Laboratory Press 2004.
2. Hogan RN, Baringer JR, Prusiner SB: **Scrapie infection diminishes spines and increases varicosities of dendrites in hamsters: a quantitative Golgi analysis.** *J Neuropathol Exp Neurol* 1987, **46**:461-473.
3. Jeffrey M, Halliday WG, Bell J, Johnston AR, MacLeod NK, Ingham C, Sayers AR, Brown DA, Fraser JR: **Synapse loss associated with abnormal PrP precedes neuronal degeneration in the scrapie-infected murine hippocampus.** *Neuropathol Appl Neurobiol* 2000, **26**:41-54.
4. Prusiner SB: **Novel proteinaceous infectious particles cause scrapie.** *Science* 1982, **216**:136-144.
5. Mironov A Jr, Latawiec D, Wille H, Bouzamondo-Bernstein E, Legname G, Williamson RA, Burton D, DeArmond SJ, Prusiner SB, Peters PJ: **Cytosolic prion protein in neurons.** *J Neurosci* 2003, **23**:7183-7193.
6. Linden R, Martins VR, Prado MA, Cammarota M, Izquierdo I, Brentani RR: **Physiology of the prion protein.** *Physiol Rev* 2008, **88**:673-728.
7. Büeler H, Aguzzi A, Sailer A, Greiner RA, Autenried P, Aguet M, Weissmann C: **Mice devoid of PrP are resistant to scrapie.** *Cell* 1993, **73**:1339-1347.
8. Soto C: **Unfolding the role of protein misfolding in neurodegenerative diseases.** *Nat Rev Neurosci* 2003, **4**:49-60.
9. Riemer C, Neidhold S, Burwinkel M, Schwarz A, Schultz J, Krätzschmar J, Mönning U, Baier M: **Gene expression profiling of scrapie-infected brain tissue.** *Biochem Biophys Res Commun* 2004, **323**:556-564.
10. Brown AR, Rebus S, McKimmie CS, Robertson K, Williams A, Fazakerley JK: **Gene expression profiling of the preclinical scrapie-infected hippocampus.** *Biochem Biophys Res Commun* 2005, **334**:86-95.
11. Skinner PJ, Abbassi H, Chesebro B, Race RE, Reilly C, Haase AT: **Gene expression alterations in brains of mice infected with three strains of scrapie.** *BMC Genomics* 2006, **7**:114.
12. Xiang W, Hummel M, Mitteregger G, Pace C, Windl O, Mansmann U, Kretzschmar HA: **Transcriptome analysis reveals altered cholesterol metabolism during the neurodegeneration in mouse scrapie model.** *J Neurochem* 2007, **102**:834-847.
13. Sorensen G, Medina S, Parchaliuk D, Phillipson C, Robertson C, Booth SA: **Comprehensive transcriptional profiling of prion infection in mouse models reveals networks of responsive genes.** *BMC Genomics* 2008, **9**:114.
14. Greenwood AD, Horsch M, Stengel A, Vorberg I, Lutzny G, Maas E, Schädler S, Erfle V, Beckers J, Schätzl H, Leib-Mösch C: **Cell line dependent RNA expression profiles of prion-infected mouse neuronal cells.** *J Mol Biol* 2005, **349**:487-500.
15. Chich JF, Schaeffer B, Bouin AP, Mouthon F, Labas V, Larramendy C, Deslys JP, Grosclaude J: **Prion infection-impaired functional blocks identified by proteomics enlighten the targets and the curing pathways of an anti-prion drug.** *Biochim Biophys Acta* 2007, **1774**:154-167.
16. Goshima Y, Nakamura F, Strittmatter P, Strittmatter SM: **Collapsin-induced growth cone collapse mediated by an intracellular protein related to UNC-33.** *Nature* 1995, **376**:509-514.
17. Wang LH, Strittmatter SM: **A family of rat CRMP genes is differentially expressed in the nervous system.** *J Neurosci* 1996, **16**:6197-6207.
18. Byk T, Ozon S, Sobel A: **The Ulip family phosphoproteins.** *Eur J Biochem* 1998, **254**:14-24.
19. Kamata T, Subleski M, Hara Y, Yuhki N, Kung H, Copeland NG, Jenkins NA, Yoshimura T, Modi W, Copeland TD: **Isolation and characterization of a bovine neural specific protein (CRMP-2) cDNA homologous to *unc-33*, a *C. elegans* gene implicated in axonal outgrowth and guidance.** *Mol Brain Res* 1998, **54**:219-236.
20. Yoshimura T, Kawano Y, Arimura N, Kawabata S, Kikuchi A, Kaibuchi K: **GSK-3β regulates phosphorylation of CRMP-2 and neuronal polarity.** *Cell* 2005, **120**:137-149.
21. Shinagawa M, Takahashi K, Sasaki S, Doi S, Goto H, Sato G: **Characterization of scrapie agent isolated from sheep in Japan.** *Microbiol Immunol* 1985, **29**:543-551.
22. Inoue Y, Yamakawa Y, Sakudo A, Kinumi T, Nakamura Y, Matsumoto Y, Saeki K, Kamiyama T, Onodera T, Nishijima M: **Infection route-independent accumulation of splenic abnormal prion protein.** *Jpn J Infect Dis* 2005, **58**:78-82.
23. Diedrich J, Wietgrefe S, Zupancic M, Staskus K, Retzel E, Haase AT, Race R: **The molecular pathogenesis of astrogliosis in scrapie and Alzheimer's disease.** *Microb Pathog* 1987, **2**:435-442.

24. Gray BC, Skipp P, O'Connor VM, Perry VH: **Increased expression of glial fibrillary acidic protein fragments and μ-calpain activation within the hippocampus of prion-infected mice.** *Biochem Soc Trans* 2006, **34**:51-54.
25. Kumar Y, Khachane A, Belwal M, Das S, Somsundaram K, Tatu U: **ProteoMod: A new tool to quantitate protein post-translational modifications.** *Proteomics* 2004, **4**:1672-1683.
26. Zhu K, Zhao J, Lubman DM, Miller FR, Barder TJ: **Protein pI shifts due to posttranslational modifications in the separation and characterization of proteins.** *Anal Chem* 2005, **77**:2745-2755.
27. Zhuo S, Clemens JC, Hakes DJ, Barford D, Dixon JE: **Expression, purification, crystallization, and biochemical characterization of a recombinant protein phosphatase.** *J Biol Chem* 1993, **268**:17754-17761.
28. Breci LA, Tabb DL, Yates JR, Wysocki VH: **Cleavage N-terminal to proline: analysis of a database of peptide tandem mass spectra.** *Anal Chem* 2003, **75**:1963-1971.
29. Gu Y, Hamajima N, Ihara Y: **Neurofibrillary tangle-associated collapsin response mediator protein-2 (CRMP-2) is highly phosphorylated on Thr-509, Ser-518, and Ser-522.** *Biochemistry* 2000, **39**:4267-4275.
30. Yuasa-Kawada J, Suzuki R, Kano F, Ohkawara T, Murata M, Noda M: **Axonal morphogenesis controlled by antagonistic roles of two CRMP subtypes in microtubule organization.** *Eur J Neurosci* 2003, **17**:2329-2343.
31. Rogemond V, Auger C, Giraudon P, Becchi M, Auvergnon N, Belin MF, Honnorat J, Moradi-Améli M: **Processing and nuclear localization of CRMP2 during brain development induce neurite outgrowth inhibition.** *J Biol Chem* 2008, **283**:14751-14761.
32. Bretin S, Reibel S, Charrier E, Maus-Moatti M, Auvergnon N, Thevenoux A, Glowinski J, Rogemond V, Prémont J, Honnorat J, Gauchy C: **Differential expression of CRMP1, CRMP2A, CRMP2B, and CRMP5 in axons or dendrites of distinct neurons in the mouse brain.** *J Comp Neurol* 2005, **486**:1-17.
33. Quinn CC, Chen E, Kinjo TG, Kelly G, Bell AW, Elliott RC, McPherson PS, Hockfield S: **TUC-4b, a novel TUC family variant, regulates neurite outgrowth and associates with vesicles in the growth cone.** *J Neurosci* 2003, **23**:2815-2823.
34. Bretin S, Rogemond V, Marin P, Maus M, Torrens Y, Honnorat J, Glowinski J, Prémont J, Gauchy C: **Calpain product of WT-CRMP2 reduces the amount of surface NR2B NMDA receptor subunit.** *J Neurochem* 2006, **98**:1252-1265.
35. Zhang Z, Ottens AK, Sadasivan S, Kobeissy FH, Fang T, Hayes RL, Wang KK: **Calpain-mediated collapsin response mediator protein-1, -2, and -4 proteolysis after neurotoxic and traumatic brain injury.** *J Neurotrauma* 2007, **24**:460-472.
36. Touma E, Kato S, Fukui K, Koike T: **Calpain-mediated cleavage of collapsin response mediator protein (CRMP)-2 during neurite degeneration in mice.** *Eur J Neurosci* 2007, **26**:3368-3381.
37. Kobeissy FH, Ottens AK, Zhang Z, Liu MC, Denslow ND, Dave JR, Tortella FC, Hayes RL, Wang KK: **Novel differential neuroproteomics analysis of traumatic brain injury in rats.** *Mol Cell Proteomics* 2006, **5**:1887-1898.
38. Jiang SX, Kappler J, Zurakowski B, Desbois A, Aylsworth A, Hou ST: **Calpain cleavage of collapsin response mediator proteins in ischemic mouse brain.** *Eur J Neurosci* 2007, **26**:801-809.
39. Katano T, Mabuchi T, Okuda-Ashitaka E, Inagaki N, Kinumi T, Ito S: **Proteomic identification of a novel isoform of collapsin response mediator protein-2 in spinal nerves peripheral to dorsal root ganglia.** *Proteomics* 2006, **6**:6085-6094.
40. Tompa P, Buzder-Lantos P, Tantos A, Farkas A, Szilágyi A, Bánóczi Z, Hudecz F, Friedrich P: **On the sequential determinants of calpain cleavage.** *J Biol Chem* 2004, **279**:20775-20785.
41. Cuerrier D, Moldoveanu T, Davies PL: **Determination of peptide substrate specificity for μ-calpain by a peptide library-based approach: the importance of primed side interactions.** *J Biol Chem* 2005, **280**:40632-40641.
42. Auvergnon N, Reibel S, Touret M, Honnorat J, Baron T, Giraudon P, Bencsik A: **Altered expression of CRMPs in the brain of bovine spongiform encephalopathy-infected mice during disease progression.** *Brain Res* 2009, **1261**:1-6.
43. Stenmark P, Ogg D, Flodin S, Flores A, Kotenyova T, Nyman T, Nordlund P, Kursula P: **The structure of human collapsin response mediator protein 2 a regulator of axonal growth.** *J Neurochem* 2007, **101**:906-917.
44. Kim CL, Umetani A, Matsui T, Ishiguro N, Shinagawa M, Horiuchi M: **Antigenic characterization of an abnormal isoform of prion protein using a new diverse panel of monoclonal antibodies.** *Virology* 2004, **320**:40-51.
45. Shevchenko A, Wilm M, Vorm O, Mann M: **Mass spectrometric sequencing of proteins from silver-stained polyacrylamide gels.** *Anal Chem* 1996, **68**:850-858.
46. Yanagisawa Y, Sato Y, Asahi-Ozaki Y, Ito E, Honma R, Imai J, Kanno T, Kano M, Akiyama H, Sata T, Shinkai-Ouchi F, Yamakawa Y, Watanabe S, Katano H: **Effusion and solid lymphomas have distinctive gene and protein expression profiles in ananimal model of primary effusion lymphoma.** *J Pathol* 2006, **209**:464-473.
47. **Protein Prospector program developed by the University of California, San Francisco, Mass Spectrometry Facility.** [http://prospector.ucsf.edu/prospector/cgi-bin/msform.cgi?form=msfitstandard].
48. Perkins DN, Pappin DJ, Creasy DM, Cottrell JS: **Probability-based protein identification by searching sequence databases using mass spectrometry data.** *Electrophoresis* 1999, **20**:3551-3567.
49. **ExPaSy Protemics Server, Compute pI/MW tool.** [http://kr.expasy.org/tools/pi_tool.html].
50. Obenauer JC, Cantley LC, Yaffe MB: **Scansite 2.0: Proteome-wide prediction of cell signaling interactions using short sequence motifs.** *Nucleic Acids Res* 2003, **31**:3635-3641.
51. Nielsen AL, Holm IE, Johansen M, Bonven B, Jørgensen P, Jørgensen AL: **A new splice variant of glial fibrillary acidic protein, GFAPε, interacts with the presenilin proteins.** *J Biol Chem* 2002, **277**:29983-29991.
52. Pappin DJ, Hojrup P, Bleasby AJ: **Rapid identification of proteins by peptide-mass fingerprinting.** *Curr Biol* 1993, **3**:327-332.

doi:10.1186/1477-5956-8-53
Cite this article as: Shinkai-Ouchi *et al.*: **Identification and structural analysis of C-terminally truncated collapsin response mediator protein-2 in a murine model of prion diseases.** *Proteome Science* 2010 **8**:53.

FULL PAPER *Clinical Pathology*

Proteasome Activity and Biological Properties of Normal Prion Protein: A Comparison between Young and Aged Cattle

Yumi YOSHIOKA[1], Naotaka ISHIGURO[1]* and Yasuo INOSHIMA[1]

[1]*Laboratory of Food and Environmental Hygiene, Department of Veterinary Medicine, Faculty of Applied Biological Sciences, Gifu University, 1–1 Yanagido, Gifu 501–1193, Japan*

(Received 10 April 2010/Accepted 18 July 2010/Published online in J-STAGE 2 August 2010)

ABSTRACT. Atypical bovine spongiform encephalopathy (atypical BSE) has recently been identified in several countries including Japan. Most cases of atypical BSE have been reported in cattle older than 8 years of age. To clarify the association between age and occurrence of atypical BSE, we investigated both the physiological properties and amount of cellular prion protein (PrP^C) in brain homogenates from young and aged cattle by enzyme-linked immunosorbent assay and immunoblotting. The amount of PrP^C in the brain homogenates was not significantly different between young and aged cattle, but the amount in the detergent-insoluble fraction in the aged cattle was significantly higher than that of young cattle. Significant differences were observed in neither of the glycosylation forms nor in proteinase K sensitivity in young and aged cattle. Age-related changes included deposition of lipofuscin pigment and a decrease of 33% in proteasome activity in the brains of aged cattle compared to that of young cattle.

KEY WORDS: atypical BSE, brain homogenate, cattle, prion, proteasome.

J. Vet. Med. Sci. 72(12): 1583–1587, 2010

Prion diseases, also known as transmissible spongiform encephalopathies (TSE), are a group of fatal neurodegenerative disorders caused by accumulation of the proteinase K (PK)-resistant pathogenic isoform (PrP^{res}) in the host cellular prion protein (PrP^C) [17]. TSE, which have been found in humans and other mammalian species, include bovine spongiform encephalopathies (BSE) in cattle and scrapie in sheep and goats. Only one strain of BSE prion was originally thought to exist, in contrast to the many different scrapie strains found around the world [3]. Recently, however, a strain of atypical BSE, which is different from the classical BSE, was independently reported in Italy [5], France [1], and Japan [21]. Atypical BSE is classified into two different types: H-type, characterized by a higher molecular mass associated with the unglycosylated protein band, and L-type or a bovine amyloidotic spongiform encephalopathy (BASE), characterized by an unglycosylated protein band with a lower molecular mass and the predominance of a monoglycosylated band [1, 5].

To date, more than 40 cases of atypical BSE, including 2 cases in Japan [13, 21], have been documented globally through active surveillance systems. Most atypical BSE cases have occurred in cattle over 8 years of age, although classical BSE cases occur mostly in animals between 4 and 6 years of age. This indicates that atypical BSE might be associated with cattle age or age-related retrogressions such as proteasome activity. However, the biochemical properties and expression of PrP^C in the brain of aged cattle remain largely unclear.

To clarify the existence of any relationship between cattle age and occurrence of atypical BSE, the physiological properties and amount of PrP^C expression in brain homogenates were compared between young and aged cattle. Relative expressions of PrP^C in brain homogenates were not significantly different between the young and aged cattle, but the amount of detergent-insoluble PrP^C fraction in the aged cattle was slightly higher than that of the young cattle. The activity of proteasomes in the brain of aged cattle decreased by about 33% compared to that of young cattle, and deposition of lipofuscin pigment increased with advancing age.

* CORRESPONDENCE TO: ISHIGURO, N., Laboratory of Food and Environmental Hygiene, Department of Veterinary Medicine, Faculty of Applied Biological Sciences, Gifu University, 1–1 Yanagido, Gifu 501–1193, Japan.
e-mail: ishiguna@gifu-u.ac.jp

MATERIALS AND METHODS

Brain samples: The medulla oblongatae of bovine brains from 52 young healthy cattle (age: 20–35 months, Holstein) were obtained from the Gifu Prefectural Office of Meat Inspection in Japan. The medulla oblongatae from 63 aged healthy cattle (age: ≥120 months, Holstein) were obtained from the Matsumoto Meat Inspection Center in Japan. All medulla oblongatae samples were tested negative for BSE according to enzyme-linked immunosorbent assay (ELISA) kit. Medulla oblongatae from three young and three aged cattle were fixed in 10% formalin for histological analysis. The remaining samples were kept frozen at −80°C until use in ELISA and immunoblotting analyses.

Preparation of brain homogenate and fractionation: Ten percent (w/v) of brain homogenates from obex regions were prepared in 5 m*l* of lysis buffer [10 mM Tris-HCl pH 7.5, 150 mM NaCl, 0.5% nonidet P-40 (NP-40), 1.25 mM EDTA pH 8.0 and 0.5% sodium deoxycholate] on ice by means of a pestle, as described by Yuan *et al.* [23]. The brain homogenates were centrifuged at 2,500 rpm (570 × *g*) for 10 min at 4°C to collect supernatant, designated as the S1 fractions. The S1 fractions were further centrifuged at

50,000 rpm (100,000 × *g*) in an Optima TLX Ultracentrifuge with a TLA100.3 rotor (Beckman Coulter, Fullerton, CA, U.S.A.) for 1 hr at 4°C. After ultracentrifugation, the detergent-soluble (S2) fraction and the detergent-insoluble (P2) fraction were separated. The S2 fractions were concentrated with a 4-fold volume of methanol at −20°C for 30 min, and then the S2 and P2 fractions were resuspended in the buffer (10 mM Tris-HCl pH7.5 and 150 mM NaCl). Protein concentrations in the S1, S2 and P2 fractions were determined by spectrophotometer and a DC protein assay kit (Bio-Rad Laboratories, Hercules, CA, U.S.A.).

20S proteasome activity assay: The proteasome activity in the S1 fractions of brain homogenates from both young and aged cattle were measured with a 20S proteasome activity assay kit (Chemicon International, Temecula, CA, U.S.A.) according to the manufacturer's instructions. The assay kit works by detecting fluorophore 7-amino-4-methylcoumarin (AMC) after it is cleaved from the labeled substrate LLVY-AMC by the hymotrypsin-like activity of cellular proteasome. Free AMC was subjected to quantified fluorescence measured with a 380/460 nm filter set with a Wallac 1420 ARVOsx Multilabel Reader (PerkinElmer, Waltham, MA, U.S.A.). To measure the proteasome activity with the inhibitors, the S1 fractions were incubated with proteasome inhibitors such as 0.1 $\mu g/\mu l$ of lactacystin.

PK digestion and deglycosylation of PrP^C: For PK (Roche Diagnostics, Mannheim, Germany) digestion of PrP^C, 25 samples were incubated with several PK concentrations ranging from 0 to 5 $\mu g/ml$ for 30 min at 37°C, and then the reaction was terminated by addition of 0.1 mM Pefabloc (Roche Diagnostics).

For deglycosylation of the PrP^C, 9 μl amounts from six samples were denatured with 1 μl of 10 × glycoprotein denaturing buffer [6% 2-Mercaptoethanol and 10% Sodium Dodecyl Sulfate (SDS)] and boiled for 10 min. Next, 2 μl of 500 mM sodium phosphate (pH 7.5), 2 μl of 10% NP-40, 4 μl of water and 2 μl of recombinant Peptide N-glycosidase F (PNGase F; Roche Diagnostics) were added and they were then incubated for 1 hr at 37°C. The PNGase F reaction was stopped by addition of 20 μl of 2 × sample buffer (25 mM Tris-HCl pH 6.8, 2% Glycerol, 1.2 mM EDTA pH 8.0, 0.016% 2-Mercaptoethanol, 0.016% Bromo phenol blue, 2% SDS and 0.096% Urea) before subjecting samples to SDS polyacrylamide gel electrophoresis (SDS-PAGE).

SDS-PAGE and immunoblotting: Samples were mixed with an equal volume of 2 × sample buffer and boiled for 10 min. Ten micrograms of proteins were separated by Tris-Glycine SDS-PAGE with 12% NuPAGE polyacrylamide gel (Invitrogen, Carlsbad, CA, U.S.A.). The size fractionated proteins on the gels were electrotransferred onto immobilon-P polyvinylidene fluoride (PVDF; Millipore, Billerica, MA, U.S.A.) membranes at 65 V for 2 hr at 4°C. Membranes were blocked with 5% nonfat milk in phosphate buffered saline plus 0.1% Tween 20 (PBST) and reacted with anti-PrP 44B1 monoclonal antibody (mAb; [12]). The samples were also reacted with two anti-PrP mAbs 110 [12] or SAF32 (Bertin, Paris, France) recognizing N-terminal octa-repeat region. The PVDF membranes were washed in PBST and then incubated with the appropriate secondary antibody conjugated with horseradish peroxidase (GE Healthcare, Buckingham, U.K.). The bands that reacted with antibodies were then visualized by enhanced chemiluminescence (ECL kit, GE Healthcare), and detected by LAS-4000UVmini lumino image analyzer using Multi-Gauge software (Fujifilm, Tokyo, Japan).

After immunodetection with anti-PrP mAb 44B1, the antibodies bound to membranes were completely stripped, and reprobed with anti-synapsin I mAb (Sigma-Aldrich, St. Louis, MO, U.S.A.) by the same procedure as described above for cellular protein.

ELISA: To estimate the quantity of glial fibrillary acidic protein (GFAP) in the brain homogenates, S1 fractions (young cattle, n=10; aged cattle, n=8) were analyzed with a RIDA SCREEN® Risk Material 10/5 ELISA (R-Biopharm AG, Darmstadt, Germany) according to the manufacturer's instructions. To determine the quantity of PrP^C in the brain homogenates from young and aged cattle, the S1 (young cattle, n=10; aged cattle, n=8) and, S2 and P2 (young cattle, n=20; aged cattle, n=45) were analyzed by FRELISA® BSE (FUJIREBIO, Tokyo, Japan). Results were examined for statistical significance with the Student's unpaired *t*-test.

Histological analysis: Formalin-fixed medulla oblongatae at the obex were defatted with alcohol and embedded in paraffin. The paraffin-embedded blocks were cut into 4-μm sections, and routinely deparaffinized, rehydrated, and then stained with hematoxylin and eosin (HE).

RESULTS

Physiological comparison of obex samples from young and aged cattle: To examine whether the proteasome activity in bovine brain is influenced by advancing age, 20S proteasome activity in brain homogenates from young and aged cattle was determined in the S1 fractions with a 20S proteasome activity assay kit. The 20S proteasome activity of the aged cattle was about 33% lower than that of the young cattle: this represents a significant difference ($P<0.01$, Fig. 1). When the samples were incubated with the lactacystin inhibitor, the proteasome activity decreased 24% in the young cattle and 26% in the aged cattle.

Histological analysis revealed deposition of lipofuscin pigment in the obex region in both the young and aged cattle, with more deposition in the aged cattle (data not shown).

Expression of PrP^C in brains of young and aged cattle: To determine the expression level of PrP^C in the brains of the aged cattle, amounts of PrP^C in the S1 fraction were examined with a FRELISA® BSE kit. The amount of PrP^C in the S1 fraction was not significantly different between the young and aged cattle (Fig. 2A). The amount of glial marker GFAP in the S1 fraction was also not significantly different between the young and aged cattle (Fig. 2B). The amount of PrP^C in the P2 fraction was significantly higher in the aged cattle than in young cattle ($P<0.05$), while the amount of PrP^C in the S2 fraction showed no significant dif-

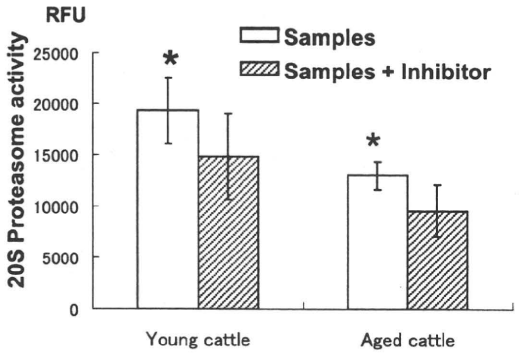

Fig. 1. Proteasome activity in brain homogenates from young and aged cattle. The 20S proteasome activity in the S1 fraction of brain homogenates from young (8 cattle: 17–24 months) and aged (8 cattle: 60–100 months) cattle was determined by a 20S proteasome activity assay kit. The 20S proteasome activity was measured with or without the lactacystin inhibitor. Histograms were obtained from 8 samples and show the mean ± SD. RFU, relative fluorescent unit, was determined by a 380/460 nm filter set with a Multilabel Reader Wallac 1420 ARVOsx. *, $P<0.01$.

ference (Fig. 2C).

The PrP^C immunoblot profile was examined with anti-PrP mAb 44B1(Fig. 3). In the S2 fraction, one major band migrating at approximately 35 kDa (lanes 2–6) is shown in Fig. 3. In the P2 fraction, one major band migrating at 26–17 KDa was detected with mAb 44B1, but not with N-terminal recognizing mAbs 110 and SAF32, suggesting that the 26–17 KDa band corresponds to the N-terminally truncated form (Fig. 3). The quantities of synapsin I in the S2 and P2 fractions were not significantly different between the young and aged cattle, although the bands reacted with anti-synapsin I were slightly different between S2 and P2 fractions.

Treatment with PNGase F and PK-sensitivity of PrP^C: After treatment with PNGase F, the PrP^C in the S2 and P2 fractions shifted mainly to the 30-kDa band corresponding to the full-length PrP^C and the 18-kDa band corresponding to an N-terminally truncated PrP^C fragments (Fig. 4). There was no significant difference in glycosylation forms between the young and aged cattle.

To examine PK sensitivity, the S2 and P2 fractions from different aged cattle were treated in either the absence or presence of 1, 1.25, 1.6, 2.5 and 5 $\mu g/\mu l$ of PK for 30 min, after which the PrP^C molecules were studied by immunoblot analysis (Fig. 5). After incubation with 5 $\mu g/\mu l$ of PK, most PrP^C in the S2 fraction was relatively digested in contrast to PrP^C in the P2 fraction. These results indicate that the S2 fraction was relatively sensitive to PK concentration in both the young and aged cattle, whereas the P2 fraction was relatively resistant to PK treatment in both the young and aged cattle.

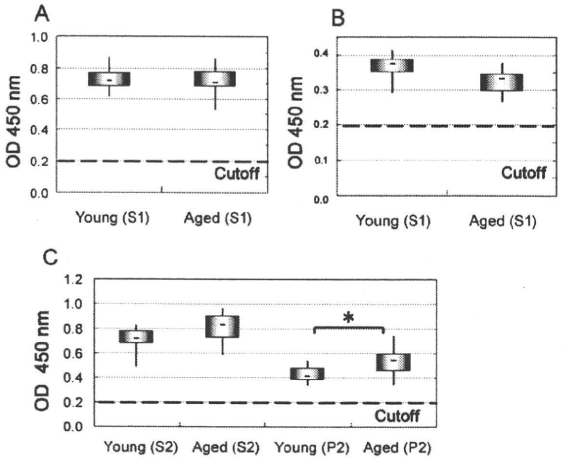

Fig. 2. Comparison of the amounts of PrP^C expression and quantity of GFAP in brain homogenates. A) The amounts of PrP^C in the S1 were detected by a FRELISA® BSE. The cutoff value was determined by the value at 0.150 plus the mean value of negative controls according to the manufacturer's instructions. Young cattle, 10 samples; Aged cattle, 8 samples. B) The quantity of GFAP was determined by a RIDASCREEN® Risk Material 10/5. Young cattle, 10 samples; Aged cattle, 8 samples. C) The amounts of PrP^C in the S2 and P2 were detected by a FRELISA® BSE. Young cattle, 20 samples; Aged cattle, 45 samples. *, $P<0.05$.

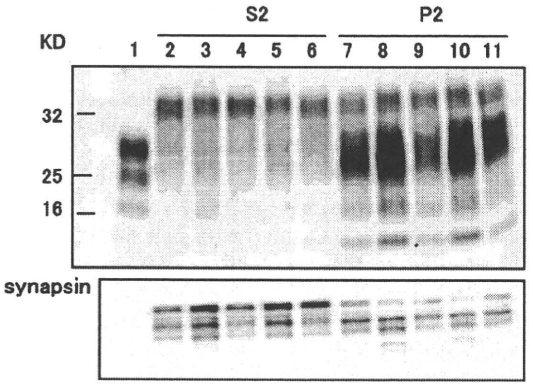

Fig. 3. The relative amounts of S2 and P2 of PrP^C in brain homogenates from young and aged cattle. The samples were separated by SDS-PAGE, transferred onto PVDF membranes and reactd with mAb 44B1. Lane 1, Scrapie (Obihiro strain) affected mouse brain; lanes 2, 4, 6, 7, 9 and 11, young cattle (20-month old); lanes 3, 5, 8 and 10, aged cattle (lanes 3 and 8, 175-month old; lanes 5 and 10, 129-month old).

DISCUSSION

To clarify the relationship between aged cattle and the occurrence of atypical BSE, we focused on the physiological properties and amount of PrP^C in brain homogenates from young and aged cattle. In this study, the brains of aged cattle (>120 months) exhibited a significant decrease in the

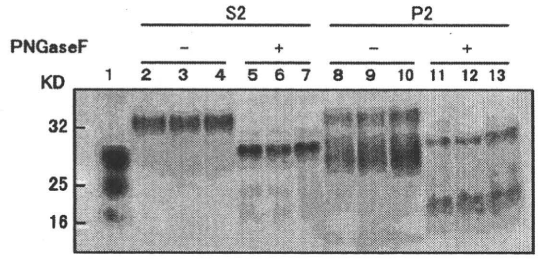

Fig. 4. Immunoblot analysis of PrP^C in brain homogenates after treatment with PNGaseF. The samples were separated by SDS-PAGE, transferred onto PVDF membranes and reacted with mAb 44B1. Molecular mass markers are indicated on the left. Lane 1, Scrapie (Obihiro strain) affected mouse brain; lanes 2, 3, 5, 6, 8, 9, 11 and 12, young cattle (20-month old); lanes 4, 7, 10 and 13, aged cattle (175-month old).

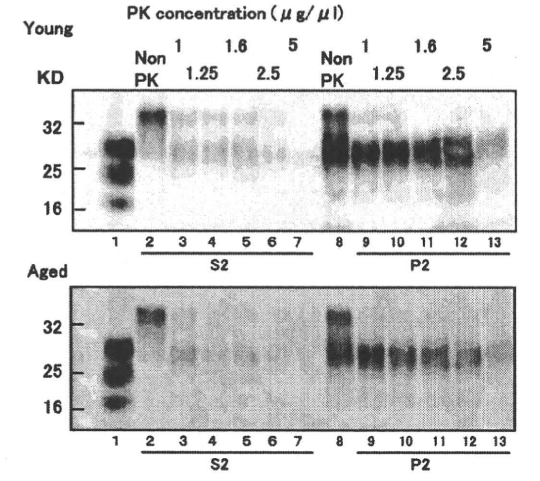

Fig. 5. Immunoblot analysis of PrP^C in brain homogenates after PK treatment. The samples after PK treatment were separated by SDS-PAGE, transferred onto PVDF membranes and reacted with mAb 44B1. Lane 1, Scrapie (Obihiro strain) affected mouse brain; S2, lanes 2–7; P2, lanes 9–13; lanes 2 and 8, non PK control.

20S proteasome activity, and deposition of lipofuscin pigment served as a sign of aging. Oxidative metabolism is essential for neurons to generate energy, because the high energy demands in neurons lead to aging vulnerability [7]. Additionally, lipofuscin contains some materials derived from lysosomal degradation; furthermore, it increases with aging [7].

We believe our study is support for the age-related decreases of protein turnover in cells. In our study, the amount of PrP^C in the detergent-insoluble (P2) fraction was significantly higher in the young than in the aged cattle (Fig. 2C), which agrees well with a decrease in protein turnover including 20S proteasome activity with aging. *In vitro* evidence has shown that the 20S proteasome selectively degrades damaged proteins following an oxidative insult [8], and is a marker of the primary mechanism for the degrading oxidized proteins [6]. Age-related decline in proteasome activity is also reported in the brain [4] and spinal cord [11].

To analyze more details of the physiological properties of PrP^C, the S1 fraction was then fractionated into detergent-soluble (S2) and detergent-insoluble (P2) proteins. PrP^C amounts in the S2 and P2 fractions of the aged cattle was slightly higher than that of young cattle, while PrP^C amount of the S1 fraction was almost same in young and aged cattle (Fig. 2A). Several experiments using proteasomal inhibitors such as MG132 and N-acetyl-leucinal-leucinal-norleucinal (ALLN) revealed that wild type PrP^C is accumulated in both detergent-soluble and -insoluble species, when cells are incubated with proteasomal inhibitors [14, 22]. In particular, the insoluble fraction includes an unglycosylated 26 kDa PrP^C molecules with a protease-resistant core [14, 22]. Thus in our study, the remarkable accumulation of PrP^C in the P2 fraction of the aged cattle may be caused by the significant decreases in the 20S proteasome activity (Figs. 1 and 2). In our study, the P2 samples from young and aged cattle were relatively resistant to PK treatement. However, it is not clear how the physiological properties of PrP^C such as PK resistance and accumulation of PrP^C in the P2 fraction of the aged cattle are associated with occurrence of atypical BSE. In the future, to elucidate the relationship between expression of PrP^C and occurrence of atypical BSE, brain samples from atypical BSE need to be characterized directly.

We found influences of aging on neither of the glycosylation forms nor on PK sensitivity in the bovine PrP^C. However, Goh *et al.* described both an increasing prevalence in the complex oligosaccharides in PrP^C from aged mice and an absence of any relationship between aging and PK sensitivity of mouse PrP^C [10]. We conclude that age-related physiological changes in PrP^C are not the same in cattle and mice. Likewise, Salès *et al.* reported that PrP^C expression increase with age in the brain of hamsters [18], while in the present study, the amount of PrP^C in the S1 fractions were similar in young and aged cattle, suggesting that PrP^C expression may not change drastically with age in the brains of cattle. Again, we conclude interspecies differences.

The present study provides insight into possible explanations for the correlation between cattle age and occurrence of atypical BSE. Perhaps aging should not be considered strictly as an influence on PrP^C, but also as an influence on variable structures and functions of the brain due through genetic and environmental mechanisms. Despite the plethora of research on neurodegenerative diseases associated with aging in humans, such as Alzheimer's and Parkinson's diseases, questions concerning aging still remain [7]. Mitochondrial dysfunction is thought to be a key factor in age-related diseases of humans [19] and should therefore be investigated in the cattle. Biological relationships between aging and PrP^C, including antioxidant-like activity [2], synaptic transmission [15], and the expression of PrP^C exposure

to oxidative stress in the aged mice [20], have also been reported. Thus, it is conceivable that PrP^{C} plays a role in protecting neurons from the effects of cellular stress.

The origin and mechanisms of the occurrence atypical BSE remains unknown, as with classical BSE. Only one cases of atypical BSE have been reported in young cattle, while classical BSE occurred in aged cattle in Japan [13, 21]. It is very difficult to precisely estimate the influences of age on atypical and classical BSE cases. Atypical BSE and classical BSE display unique incubation periods, PrP^{res} deposition patterns, and histological lesions [9, 16]. However, because the onset of BSE is affected by exposure dose of BSE agent and host susceptibility, it is difficult to estimate the infection time for both classical and atypical BSE cases. There is a possibility that atypical BSE agents could infect young cattle and reside within the body for long periods before symptoms of BSE appears in aged cattle. In addition, the low prevalence of atypical BSE identified through mainly active surveillance means that whole brains are not often available for examination. Thus the need remains for detailed sampling of the brain, with the exception the obex region, to determine the etiology of atypical BSE.

ACKNOWLEDGMENTS. We would like to thank the staff of the local Meat Inspection Centers in Gifu and Nagano Prefectures for providing cattle brain samples. This study was supported in part by a Grant-in-Aid for Scientific Research (B) (No.17380180) from the Ministry of Education, Cultures, Sports, Science and Technology of Japan, and by a grant from the Ministry of Health, Labour and Welfare of Japan.

REFERENCES

1. Biacabe, A. G., Laplanche, J. L., Ryder, S. and Baron, T. 2004. Distinct molecular phenotypes in bovine prion diseases. *EMBO Rep.* **5**: 110–115.
2. Brown, D. R., Wong, B. S., Hafiz, F., Clive, C., Haswell, S. J. and Jones, I. M. 1999. Normal prion protein has an activity like that of superoxide dismutase. *Biochem. J.* **344**: 1–5.
3. Bruce, M. E. and Dickinson, A. G. 1987. Biological evidence that scrapie agent has an independent genome. *J. Gen. Virol.* **68**: 79–89.
4. Carney, J. M., Starke-Reed, P. E., Oliver, C. N., Landum, R. W., Cheng, M. S., Wu, J. F. and Floyd, R. A. 1991. Reversal of age-related increase in brain protein oxidation, decrease in enzyme activity, and loss in temporal and spatial memory by chronic administration of the spin-trapping compound N-tert-butyl-alpha-phenylnitrone. *Proc. Natl. Acad. Sci. U.S.A.* **88**: 3633–3636.
5. Casalone, C., Zanusso, G., Acutis, P., Ferrari, S., Capucci, L., Tagliavini, F., Monaco, S. and Caramelli, M. 2004. Identification of a second bovine amyloidotic spongiform encephalopathy: molecular similarities with sporadic Creutzfeldt-Jakob disease. *Proc. Natl. Acad. Sci. U.S.A.* **101**: 3065–3070.
6. Davies, K. J. 2001. Degradation of oxidized proteins by the 20S proteasome. *Biochemical* **83**: 301–310.
7. Esiri, M. M. 2007. Aging and brain. *J. Pathol.* **211**: 181–187.
8. Ferrington, D. A., Sun, H., Murray, K. K., Costa, J., Williams, T. D., Bigelow, D. J. and Squier, T. C. 2001. Selective degradation of oxidized calmodulin by the 20S proteasome. *J. Biol. Chem.* **276**: 937–943.
9. Fukuda, S., Iwamaru, Y., Imamura, M., Masujin, K., Shimizu, Y., Matsuura, Y., Shu, Y., Kurachi, M., Kasai, K., Murayama, Y., Onoe, S., Hagiwara, K., Sata, T., Mohri, S., Yokoyama, T. and Okada, H. 2009. Intraspecies tramsmission of L-type-like bovine spongiform encephalopathy detected in Japan. *Microbiol. Immunol.* **53**:704–707.
10. Goh, A. X., Li, C., Sy, M. S. and Wong, B. S. 2007. Altered prion protein glycosylation in the aging mouse brain. *J. Neurochem.* **100**: 841–854.
11. Keller, J. N., Huang, F. F. and Markesbery, W. R. 2000. Decreased levels of proteasome activity and proteasome expression in aging spinal cord. *Neuroscience* **98**: 149–156.
12. Kim, C. L., Umetani, A., Matsui, T., Ishiguro, N., Shinagawa, M. and Horiuchi, M. 2004. Antigenic characterization of an abnormal isoform of prion protein using a new diverse panel of monoclonal antibodies. *Virology* **320**: 40–51.
13. Hagiwara, K., Yamakawa, Y., Sato, Y., Nakamura, Y., Tobiume, M., Shinagawa, M. and Sata, M. 2007. Accumulation of mono-glycosylated form-rich, plaque-forming PrP^{Sc} in the second atypical bovine spongiform encephalopathy case in Japan. *Jpn. J. Infect. Dis.* **60**: 305–308.
14. Ma, J. and Lindquist, S. 2001. Wild-type PrP and a mutant associated with prion disease are subject to retrograde transport and proteasome degaradation. *Proc. Natl. Acad. Sci. U.S.A.* **98**: 14955–14960.
15. Maglio, L. E., Martins, V. R., Izquierdo, I. and Ramirez, O. A. 2006. Role of cellular prion protein on LTP expression in aged mice. *Brain Res.* **1097**: 11–18.
16. Masujin, K., Shu, Y., Yamakawa, Y., Hagiwara, K., Sata, T., Matsuura, Y., Iwamaru, Y., Imamura, M., Okada, H., Mohri, S. and Yokoyama, T. 2008. Biological and biochemical characterization of L-type-like bovine spongiform encephalopathy (BSE) detected in Japanese black beef cattle. *Prion* **2**: 123–128.
17. Prusiner, S. B. 1982. Novel proteinaceous infectious particles cause scrapie. *Science* **216**: 136–144.
18. Salés, N., Hässing, R., Rodolfo, K., Di Giamberardino, L., Traiffort, E., Ruat, M., Frétier, P. and Moya, K. L. 2002. Developmental expression of the cellular prion protein in elongating axons. *Eur. J. Neurosci.* **15**: 1163–1177.
19. Vanitallie, T. B. 2008. Parkinson disease: primacy of age as a risk factor for mitochondrial dysfunction. *Metabolism* **57**: 50–55.
20. Williams, W. M., Stadtman, E. R. and Moskovitz, J. 2004. Ageing and exposure to oxidative stress in vivo differentially affect cellular levels of PrP^{c} in mouse cerebral microvessels and brain parenchyma. *Neuropathol. Appl. Neurobiol.* **30**: 161–168.
21. Yamakawa, Y., Hagiwara, K., Nohtomi, K., Nakamura, Y., Nishijima, M., Higuchi, Y., Sato, Y. and Sata, T. 2003. Atypical proteinase K-resistant prion protein (PrP^{res}) observed in an apparently healthy 23-month-old Holstein steer. *Jpn. J. Infect. Dis.* **56**: 221–222.
22. Yedidia, Y., Horonchik, L., Tzaban, S., Yanai, A. and Taraboulos, A. 2001. Proteasomes and ubiquitin are involved in the turnover of the wild-type prion protein. *EMBO J.* **20**: 5383–5391.
23. Yuan, J., Xiao, X., Mcgeehan, J., Dong, Z., Cali, I., Fujioka, H., Kong, Q., Kneale, G., Gambetti, P. and Zou, W.-Q. 2006. Insoluble aggregates and protease-resistant conformers of prion protein in uninfected human brains. *J. Biol. Chem.* **281**: 34848–34858.

Biochemical and Biophysical Research Communications 397 (2010) 706–710

Contents lists available at ScienceDirect

Biochemical and Biophysical Research Communications

journal homepage: www.elsevier.com/locate/ybbrc

Intron 1 mediated regulation of bovine prion protein gene expression: Role of donor splicing sites, sequences with potential enhancer and suppressor activities

Walid Elmonir [a,b], Yasuo Inoshima [a], Ahmed Elbassiouny [b], Naotaka Ishiguro [a,*]

[a] Laboratory of Food and Environmental Hygiene, Department of Veterinary Medicine, Faculty of Applied Biological Science, Gifu University, Gifu 501-1193, Japan
[b] Laboratory of Hygiene and Preventive Medicine, Faculty of Veterinary Medicine, Kafr Elsheikh University, Kafr Elsheikh, Egypt

ARTICLE INFO

Article history:
Received 24 May 2010
Available online 8 June 2010

Keywords:
Prion
Promoter
Intron 1
Splicing

ABSTRACT

Prion protein plays a key role in the pathogenesis of transmissible spongiform encephalopathies. Because changes in expression of the prion protein gene (*PRNP*) alter the incubation time and severity of prion diseases. Our previous work revealed a strong association between the promoter (spanning base pairs (bp) −88 to −30) and intron 1 (spanning bp +114 to +892) that leads to optimum expression of the bovine *PRNP*. Here, we employed two mutation analysis strategies (deletion and insertion) and two reporter assay systems (luciferase and GFP expression) to define the regulatory domains within intron 1 and further elucidate its role in regulating the promoter activity of the bovine prion protein gene. We identified DNA sequences with potential suppressor and enhancer activities within the 5′ end of intron 1. Moreover stability analyses for *PRNP* mRNAs demonstrated that splicing sites and mechanism are critical for bovine *PRNP* expression.

1. Introduction

Bovine spongiform encephalopathy (BSE) is one of the transmissible spongiform encephalopathies (TSEs). The presence of cellular prion protein (PrP) is crucial for the development, transmission, and resulting neurotoxicity of TSEs [1]. The expression level of the prion protein gene (*PRNP*) affects the disease profile, as animal models show that both knockout and low expression of *PRNP*, respectively, effectively abolish or reduce susceptibility to TSEs [2,3], while high expression is associated with susceptibility and shortened incubation time for development of the disease [4].

The genetic susceptibility of cattle to BSE is associated with polymorphisms in the regulatory region of the PRNP and the level of its expression [5–7]. The lack of any expression in mice transgenic for an intron-less PRNP highlights the importance of intron 1 for PRNP expression [8]. Polymorphisms in intron 1 are linked to expression of bovine PRNP, as well as susceptibility to BSE. Among these, 12-bp insertion and/or deletion (indel) polymorphism in intron 1 showed a significant association with BSE susceptibility [6,9].

Exon 1 was shown to be associated with suppression of *PRNP* expression [7], while exons 2 and 3 (containing the ORF) play no significant role in the activity of the bovine *PRNP* promoter [7,10].

In this study, we investigated the regulatory domains within intron 1, including alternative exon 1 and its interaction with the promoter region, to ascertain how it effects bovine *PRNP* expression. We defined sequences with suppressor and enhancer properties in the 5′ end of intron 1, and found a strong association between the mechanism of splicing and activity of the bovine *PRNP* promoter.

2. Materials and methods

2.1. Cell culture

CKT-1 cells (bovine fibroblast-like epithelial cells) [5] were cultured in Dulbecco's modified Eagle's medium (DMEM) with 5% fetal calf serum (FCS). L929 (mouse fibroblast cells) and GT 1–7 (mouse hypothalamic neuronal cells) cell lines were grown in DMEM with 10%FCS. Cells were maintained at 37 °C and 5% CO_2 in a humidified incubator.

2.2. Plasmid constructs

Two cloned constructs from our previous study [5] were used as controls. The positive control was pBPrPCAT-5, consisting of an inserted segment from bp −409 to +2527 (*PRNP* promoter, exon 1, intron 1, and part of exon 2) cloned into the basic chloramphenicol acetyl transferase (CAT) reporter plasmid, which showed almost full promoter activity using CAT assay [5]. As a negative control, we used pBPrPCAT-13, in which a segment of the *PRNP* promoter

* Corresponding author. Address: Yanagido 1-1, Gifu, 501-1193, Japan. Fax: +81 58 293 2864.
E-mail address: Ishiguna@gifu-u.ac.jp (N. Ishiguro).

0006-291X/$ - see front matter © 2010 Elsevier Inc. All rights reserved.
doi:10.1016/j.bbrc.2010.06.014

from bp +114 to +892 was deleted by digestion with *Eag*I. The insert promoter segments of both constructs were amplified by PCR using LA Taq polymerase (Takara Bio, Ohtsu, Japan) with the addition of a *Xho*I restriction site at the 5′ end and addition of a *Bgl*II restriction site at the 3′ end for cloning. The following primers were used for cloning constructs (new restriction site sequences indicated by bold and underline): Forward 5′-CCCCCC**CTCGAG**GCCTCAAATTTTAATCTGAAAATT-3′ (for *Xho*I), and Reverse 5′-GGAGGA**AGATCT**GTTCAGTTTTCAAATATATTCAG-3′ (for *Bgl*II).

All primers were designed using GENETYX Ver. 8.2.2 software (GENETYX, Tokyo, Japan), and the primer sequences were based on the sequence of bovine *PRNP* (GenBank accession number: D26150). Reaction mixtures for PCR contained the following: 1 μl of DNA template (<1 μg), 5 μl of 10X LA PCR Buffer II (Mg^{2+} free), 5 μl of 25 mM $MgCl_2$, 8 μl of dNTP mix (2.5 mM each), 0.5 μl of LA taq polymerase (5 units/μl), 1 μl of each forward and reverse primer (10 pmol/μl), and sterilized distilled water to a final volume of 50 μl. Thermal cycling conditions were as follows: 94 °C for 1 min followed by 94 °C for 30 s, 55 °C for 1 min, and 72 °C for 3 min (30 cycles), followed by 7 min at 72 °C. Amplified PCR products with modified ends were used for further mutagenesis and were cloned into either luciferase reporter plasmids or green fluorescent protein (GFP) expression plasmids for expression assays.

2.3. Mutagenesis constructs

Deletion mutagenesis. Deletion mutagenesis by overlap extension PCR was carried out as described [11]. Two PCR products representing the flanking regions of the sequence to be deleted were prepared first: a *Xho*I product (before the deletion segment) and a *Bgl*II product (after the deletion segment). Each PCR reaction involved one modified primer specific for the region to be deleted and one of the original amplification primers: *Xho*I for the forward direction and *Bgl*II for the reverse direction. The modified primers consisted of a 30-nucleotide sequence derived from one flank of the segment to be deleted and a 12-nucleotide sequence from the opposite flank (Suppl. Table 1). The PCR reactions were carried out using LA Taq polymerase with the same reaction mixture and under the same thermal cycling conditions described above. In the subsequent step, 5 μl of each of the two flanking region PCR products were used as templates for an overlap ligation PCR containing the outermost primer pair (*Xho*I forward and *Bgl*II reverse) using LA Taq polymerase. Stepwise deletions of various length segments of the amplified promoter region of clone pBPrPCAT-5 were carried out (Fig. 1A).

Insertion mutagenesis. Two *Nde*I restriction sites were added to the ends of amplicons of chosen insert segments of bovine *PRNP* using *Nde*I linkers (New England Biolabs, Beverly, MA) according to the manufacturer's instructions. PCR products digested with *Nde*I were reinserted in the *Nde*I site at bp +1088 of clone 13luc (See also Fig. 1A). The primers used in amplification of the recovered insert segments were listed in Suppl. Table 2. Clones 36 and 37 were constructed by insertion of chemically synthesized DNA segments from bp +129 to +203, and bp +203 to +313, respectively.

2.4. Sequencing

DNA sequencing was conducted to confirm the precise insertion/deletion mutation of the modified promoter segment with no change in flanking *PRNP* sequences. Sequencing analysis was carried out using a BigDye® Terminator v3.1 Cycle Sequencing Kit and an ABI PRISM 310 Genetic Analyzer (Applied Biosystems, Foster city, CA) according to the manufacturer's instructions.

2.5. Reporter assay systems

Luciferase reporter assay. Cell lines were seeded into a 24-well plate, and plasmid constructs were transfected with Lipofectamin LTX and PLUS reagents (Invitrogen, Carlsbad, CA) according to manufacturer's instructions and incubated for 48 h. Luciferase reporter assays were carried out using a Dual-Luciferase Reporter Assay system (Promega, Madison, WI) according to manufacturer's instructions. The firefly luciferase activity was determined by measuring the relative luminescence units (RLU) using a manual luminometer (Bioorbit, Turku, Finland). Luciferase assay results were normalized for each clone by dividing the firefly luciferase reporter RLU by the Renilla luciferase reporter RLU (co-transfected internal control). At least nine readings from three separate experiments (triplicate readings/clone/experiment) were performed for each clone.

GFP expression. Amplified PCR segments were cloned into a pGLOW-TOPO vector (Invitrogen, Carlsbad, CA) for GFP expression, according to the manufacturer's instructions. GFP expression by transfected CKT-1 cells was assessed after 24 h using a Biozero fluorescent microscope (BZ-8000-Keyence, Osaka, Japan). The intensity of fluorescence in each cell was estimated using WINROOF v.5.7 software (Mitani, Tokyo, Japan). Twenty to 50 cells of each clone were tested in each of three separate experiments.

2.6. Real-Time PCR for detection of mRNA stability

Two-step Real-Time PCR was used to compare the stability of spliced and unspliced mRNA between clones 5luc (with no modification), 13luc (lacking one splice site), 56luc (lacking both splice sites), 52luc (lacking one splice site), 53luc (retaining both splice sites), and the basal reporter vector PGL4.10 as a negative control. CKT-1 cells maintained in 6-well plates were transfected with 0.5 μg of DNA from chosen plasmids and incubated for 48 h. Total RNA was extracted from the cells using an RNeasy Mini kit (QIAGEN, Valencia, CA) according to the manufacturer's instructions. Reverse transcription into cDNA was performed using a PrimeScript II High Fidelity RT-PCR kit (Takara Bio, Ohtsu, Japan) according to the manufacturer's instructions.

Relative quantity Real-Time PCR was conducted using a Thermal Cycler Dice Real Time System and SYBR premix EX Taq II (Takara Bio, Ohtsu, Japan) according to the manufacturer's instructions. For bovine *PRNP*, two sets of primers were used: an exon-based set for detecting spliced (mature) mRNA, and an intron based set for detecting unspliced mRNA (location illustrated in Fig. 1A). The following exon-based primers were used: exon 1 Forward (5′-GCCAGTCGCTG ACAGCCGCA-3′)/Multiple Cloning Site (MCS) Reverse (5′-GGCCG CCGAGGCCAGATCTG-3′). The intron-based primers used for bovine *PRNP* were as follows: intron 1 Forward (5′-GTCAAAGTAAGATTACT CAG-3′)/Intron 1 Reverse (5′-CGTGACACTGAACTCTCCTC-3′) according to GenBank accession number: D26150. Glyceraldhyde-3-phosphate dehydrogenase (*GAPDH*) gene was used as internal control to normalize values of the tested clones. The primers used for *GAPDH* [12] were as follows: *GAPDH* Forward (5′-GGCGTGAACCACGAGAA GTATAA-3′)/*GAPDH* Reverse (5′-CCCTCCACGATGCCAAAGT-3′). The reaction mixture used for relative quantity RT-PCR was as follows: 12.5 μl SYBR premix EX Taq II (2X), 1 μl PCR Forward primer (10 μM), 1 μl PCR Reverse primer (10 μM), 2 μl template cDNA (<100 ng), and addition of dH_2O to a final volume of 25 μl. Thermal cycling conditions were 95 °C for 10 s for one cycle, followed by 40 cycles of 95 °C for 5 s, 55 °C for 10 s, and 72 °C for 20 s.

The cycle threshold (*Ct*) value was estimated for the different clones. A Δ*Ct* value was then calculated for each clone by subtracting the *Ct* value for the target sample from that of internal control sample (*GAPDH*). Expression of mRNA was evaluated by the $2^{(\Delta\Delta Ct)}$: $2^{(\Delta Ct \text{ of clone 5} - \Delta Ct \text{ of tested clone})}$ method [13]. At least three

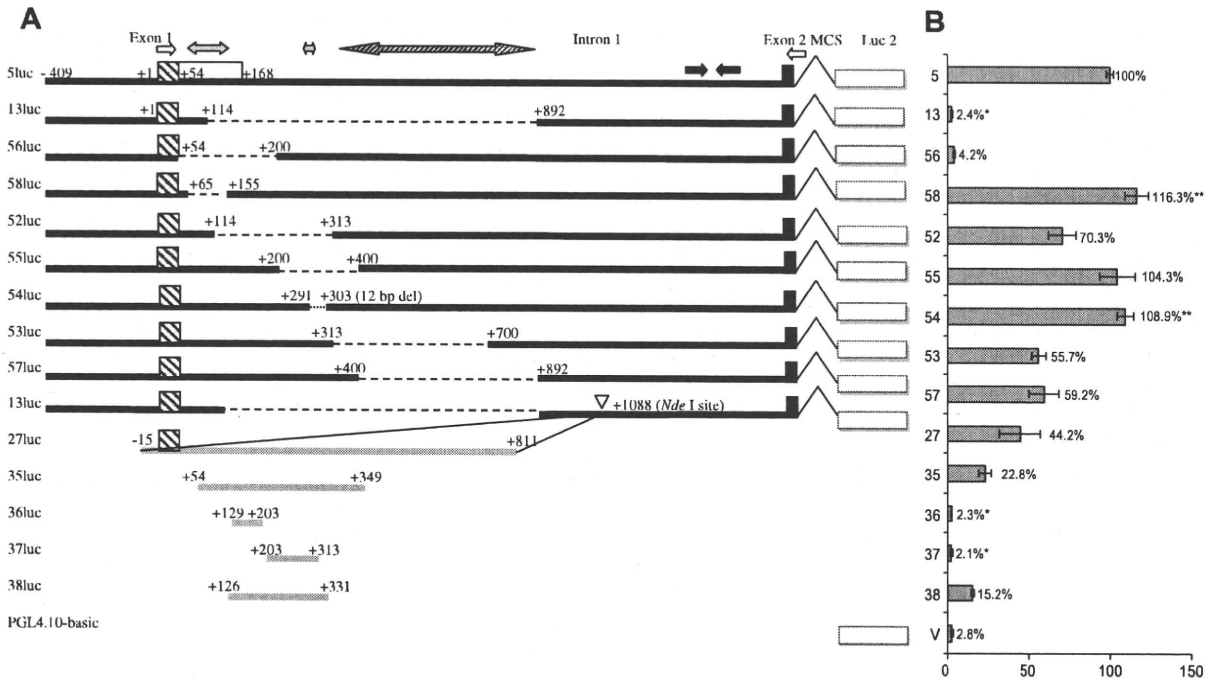

Fig. 1. Bovine *PRNP* mutation constructs used in the luciferase reporter assay. (A) Schematic diagram showing the mutant bovine *PRNP* constructs. The structure of clones 5luc and 13luc are described elsewhere [5]. Seven new deletion constructs (52luc-58luc) and five insertion constructs (27luc, 35luc, 36luc, 37luc, and 38luc) were prepared in this study. Black line: original sequence of bovine PRNP. Interrupted line: deleted sequence. Gray line: sequence inserted at *Nde*I site in intron 1. Inverted open triangle: insertion site at bp +1088 of intron 1. Hatched box: exon 1. Open box: alternative splicing region to bp +168 site. Black box: exon 2. White box: luciferase 2 reporter gene. White arrows: exon-based primers (Exon 1 Forward/Multiple Cloning Site Reverse; MCS) for real-time PCR. Black arrows: intron-based primers (Intron 1 Forward/Intron 1 Reverse) for real-time PCR. Double gray arrows: regions with putative suppressor functions. Hatched arrow: region with putative enhancer function. (B) Mean (±SD) percent luciferase activity of mutant constructs relative to original clone 5luc from three separate experiments. V: PGL4.10 basic vector. **Significantly higher than original clone 5luc ($P < 0.05$). *No significant difference compared to basal vector pGL4.10 (negative control).

separate experiments were performed for each clone. The relative quantity of *PRNP* mRNA for each clone was divided by that of *GAPDH* for normalization.

2.7. Statistical analysis

Basic statistical calculations were performed using Microsoft Excel, while AcaStat statistical v.6.2.1 software was used to perform *T*-test (two sample) and Pearson's correlation calculations.

3. Results and discussion

3.1. Defining regulatory domains within intron 1

Previously, we highlighted the importance of the bp +123 to +891 region within intron 1 for activity of the bovine *PRNP* promoter [5]. In order to assess the importance of this region to bovine *PRNP* expression, we constructed various reporter plasmids and compared their activity using two reporter vector-based systems: luciferase activity and GFP expression.

The pBPrPCAT-5 and pBPrPCAT-13 clones promoter segments were cloned into the pGL4.10 basic vector for luciferase activity analysis, and the resulting expression plasmid was designated 5luc and 13luc, respectively. Several expression plasmids were constructed by either insertion or deletion mutagenesis (Fig. 1A), and the relative luciferase activity (±standard deviation) for each was calculated (Suppl. Table 3) and shown in Fig. 1B.

The results for clones 53luc and 57luc suggest the presence of enhancer factors in the region between bp +313 and +892, because deletion of this region resulted in about a 50% reduction in promoter activity. This finding was consistent with results observed for insertion plasmid clones 27luc, 35luc, and 38luc, and implies the presence of enhancer factors in this region. The direct relationship between increased sequence length and higher promoter activity (clones 27luc, 35luc, and 38luc) indicated that the enhancer properties associated with the region after bp +313 depend upon a summation of the enhancer elements within that region. The absence of significant enhancement of expression by the sequence spanning bp +129 to +313 (clones 36luc and 37luc) may be attributed to a complete or partial lack of enhancer elements necessary for significantly influencing promoter activity. These findings may explain the lower expression of bovine *PRNP* that has been reported in cattle that have multiple single nucleotide polymorphisms (SNPs) in the region of intron 1 between bp +400 and +900 [9]. These multiple polymorphisms may alter the binding sites of enhancer elements necessary for gene expression [9]. For example, the *PRNP* enhancer sequence spanning bp +313 to +892 contains multiple binding sites for AP2, LBP-1, TCF-1, and other transcription factors that are known to activate other genes [14–16].

On the other hand, the significant over-expression ($P < 0.0001$) of clone 58luc (lacking alternative exon 1 of intron 1 which spans bp +65 to +155) compared to clone 5luc indicated the presence of suppression properties. The lack of complete recovery of promoter activity in clone 27luc agreed with these findings. The sequence in this region contains binding sites for C/EBPα, NFY, and GATA-2, each of which has been shown to suppress promoter activity in other genes [17–19]. Suppression of promoter activity by exon 1 has been reported [7], but in the previous study intron 1 was removed in order to demonstrate its suppressor activity. Our study, however, demonstrated that alternative exon 1 retained

suppressor activity even in the presence of the entire intron 1 and promoter sequence. The potential enhancer or suppressor regions in intron 1 are shown in Fig. 1A.

Another domain with suppressor properties was located in the 12 bp deleted segment of clone 54luc (site of the 12-bp indel polymorphism; bp ±291 to ±303, with putative binding site for Sp1 at bp ±297). The luciferase activity in the clone 54luc lacking 12-bp indel polymorphism site is higher than that of 5luc as shown in Fig. 1B ($P < 0.001$). The suppressor activity of the 12-bp indel polymorphism site provides a biological explanation for the strong association between 12-bp deletion polymorphisms (deleting an Sp1 binding site) and higher susceptibility to BSE infection [6,9]. Deletion of a suppressor sequence will result in higher expression of cellular PrP, which in turn is associated with a shortened incubation time and a more rapid progression of TSE [4].

The luciferase activity of clone 55luc was almost the same as clone 5luc in spite of losing the suppressor sequence of 12-bp indel polymorphism site. This may be attributed to the loss of putative enhancer elements in sequence spans bp +313 to +400 (as shown by clones 53luc and 57luc data) which compromised the suppressor effect of 12-bp indel polymorphism site.

Some of the constructed luciferase plasmids were transfected into two more cell lines (L929 and GT 1–7). The mean ± SD of luciferase activity compared to clone 5luc from at least three separate experiments are shown in Suppl. Table 3. The luciferase activity of the mutant clones were almost the same in the three cell lines (CKT-1, L929 and GT 1–7) as shown in Fig. 2. The changes in promoter activity of bovine *PRNP* mutant constructs were consistent among different cell lines.

An alternative reporter system using the GFP expression vector, driven by the deleted modified promoter segments of *PRNP*, was also employed to evaluate the same clones. Analysis of the mutant clones using GFP expression confirmed results obtained with the luciferase reporter assay for the same clones (Suppl. Table 4 and Suppl. Fig. 1).

3.2. Influence of splicing site and mechanism on the activity of the PRNP promoter

The lack of promoter activity in clone 56luc suggests that the two splicing sites (at bp +54 and bp +168) in the donor of intron 1, along with the mechanism of splicing, might be critical for promoter activity. We conducted real-time PCR experiments to investigate the possible role of the splicing mechanism on promoter activity, as well as to evaluate the stability of mRNA as a marker of promoter activity. The fold change in bovine *PRNP* mRNA expression by the $2^{(\Delta\Delta Ct)}$ method [13] was used to compare individual clones to the 5luc clone to assess promoter activity (Fig. 3). The

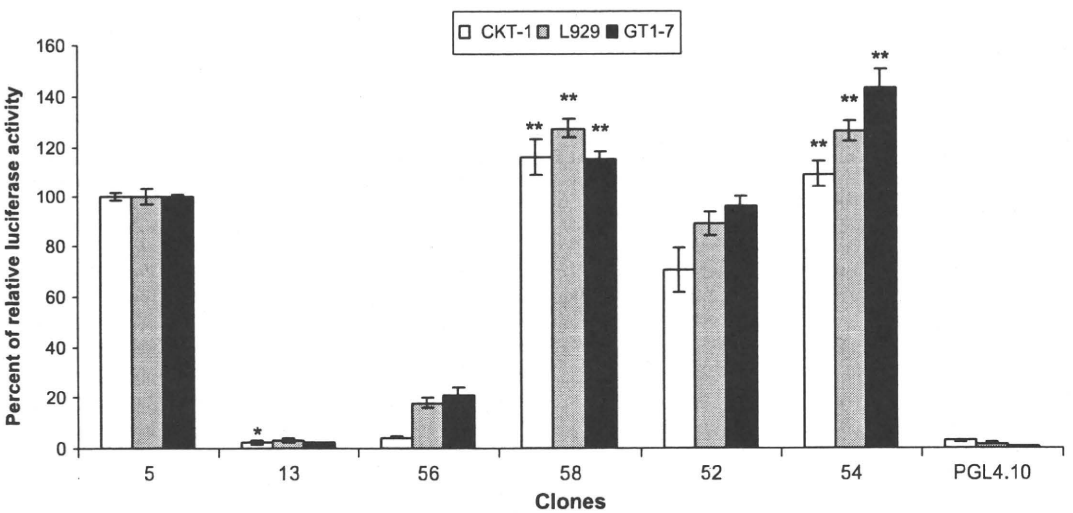

Fig. 2. Comparative luciferase activity of mutant bovine *PRNP* constructs in different cell lines. Mean (±SD) percent luciferase activity of mutant constructs relative to original clone 5luc in the corresponding cell line was obtained from three separate experiments. **Significantly higher than original clone 5luc ($P < 0.05$). *No significant difference was observed in comparison with basal vector pGL4.10 (negative control).

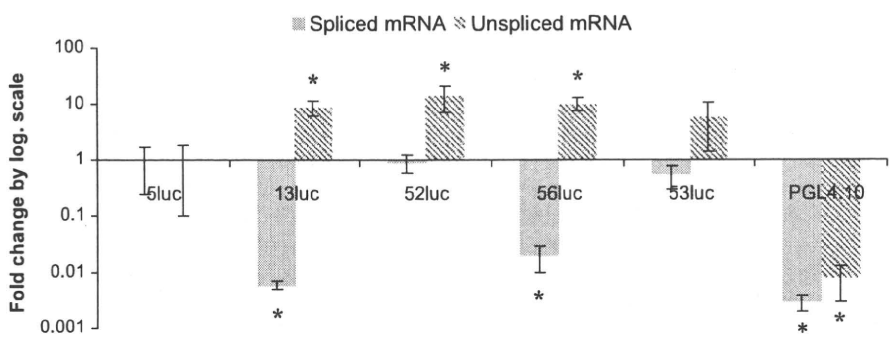

Fig. 3. Effect of splicing on fold change in bovine *PRNP* expression. Values greater than 1 indicate higher expression compared to that of original 5luc clone. Values less than 1 are indicative of lower relative expression. Results show the mean (±SD) from at least three separate experiments using the Real-Time PCR. *Significantly different expression relative to clone 5luc ($P < 0.05$).

average spliced and unspliced mRNA $2^{(\Delta\Delta Ct)}$ values (±SD) were listed in Suppl. Table 5.

The highest level of spliced mRNA was produced by clone 5luc, followed by clones 52luc and 53luc. Clones 13luc and 56luc produced significantly lower amounts of spliced mRNA compared to original clone 5luc. On the other hand, the results for clones 13luc, 56luc, and 52luc produced a significantly higher amount of unspliced mRNA compared to clone 5luc (Fig. 3). These results suggest that a deficiency of one or both splicing sites (at bp +54 and bp +168) at the donor site of intron 1 may directly affect the splicing mechanism and consequently impact *PRNP* promoter activity. Moreover, deletion of the alternative splicing site at bp +168 overwhelmed the partial deletion of the suppresser elements in clone 52luc (bp +114 to +313), resulting in the loss of approximately 30% of *PRNP* promoter activity as measured by luciferase assay. This was due to the significantly higher amount of unspliced mRNA produced as compared to the amount produced from original clone 5luc. These findings indicate that both splicing sites are critical for efficient expression of bovine *PRNP*.

Clone 53luc has higher amounts of unspliced mRNA than spliced one, even though it has intact splicing sites. The exact reason of the higher amount of unspliced mRNA in clone 53luc is not clear, but it may be attributed to the involvement of other factors that control the splicing machinery. Culler et al. [20] identified over 100 splicing elements and motifs within the introns of several genes that regulate splicing and consequently the outcome expression of these genes [20]. Therefore, the loss of partial promoter activity of bovine *PRNP* with deletion of sequence bp +313 to 700 in 53luc clone may be attributed in part to the loss of putative similar splicing elements, which influences efficiency of splicing mechanism even in presence of intact splicing sites.

There was a high positive correlation between the quantity of spliced mRNA produced by the different clones and the luciferase activity of the same clones (Pearson's correlation, $r = 0.99$); the level of spliced mRNA produced by real-time PCR was directly proportional to the level of promoter activity. Impaired splicing has been shown to suppress expression of other genes in addition to bovine *PRNP* [21].

Although Lemaire-Vieille et al. [22] found that both mRNA transcripts of exon 1 from the +53- and +168-bp sites were expressed to various degrees in almost all bovine tissues tested, their results did not clarify the role of alternative splicing in regulating bovine *PRNP* expression [20]. We found that deletion of the alternative splice site at bp +168 (clones 13luc and 52luc) resulted in an excess of unspliced mRNA which directly affected promoter activity. Alternative splicing has been shown to affect the stability of mRNA in a number of other genes [23], and we believe our results are consistent with this, in that alternative splicing of exon 1 may also impact the stability of *PRNP* mRNA.

In conclusion, we revealed two sequence regions with potential suppressor properties (the alternative exon 1 between bp +65 and +155, and the Sp1 binding site at bp +297), and one region spanning bp +313 to +892 with some enhancer influence on the expression of bovine *PRNP*. Conserved splicing sites at the intron 1 donor and the presence of an efficient splicing mechanism are necessary for optimal promoter activity.

Acknowledgments

This study was supported by a Grant-in Aid (No. 17380180) from the Ministry of Education, Science, Sports and Culture of Japan, and by a grant from the Ministry of Health, Labour and Welfare of Japan.

Appendix A. Supplementary data

Supplementary data associated with this article can be found, in the online version, at doi:10.1016/j.bbrc.2010.06.014.

References

[1] S. Brandner, A. Raeber, A. Sailer, T. Blättler, Normal host prion protein (PrPc) is required for scrapie spread within the central nervous system, Proc. Natl. Acad. Sci. USA 93 (1996) 13148–13151.
[2] H. Bueler, A. Aguzzi, A. Sailer, R.A. Greiner, P. Autenried, M. Aguet, C. Weissmann, Mice devoid of PrP are resistant to scrapie, Cell 73 (1993) 1339–1347.
[3] G. Mallucci, A. Dickinson, J. Linehan, P.C. Klöhn, S. Brandner, J. Collinge, Depleting neuronal PrP in prion infection prevents disease and reverses spongiosis, Science 302 (2003) 871–874.
[4] M. Fischer, T. Rulicke, A. Raeber, A. Sailer, Prion protein (PrP) with amino-proximal deletions restoring susceptibility of PrP knockout mice to scrapie, EMBO J. 15 (1996) 1255–1264.
[5] S. Inoue, M. Tanaka, M. Horiuchi, N. Ishiguro, M. Shinagawa, Characterization of the bovine prion protein gene: the expression requires interaction between the promoter and intron, J. Vet. Med. Sci. 59 (1996) 175–183.
[6] P. Sander, H. Hamann, C. Drogemuller, K. Kashkevich, K. Schiebel, T. Leeb, Bovine prion protein (PRNP) promoter polymorphisms modulate PRNP expression and may be responsible for differences in BSE susceptibility, J. Biol. Chem. 280 (2005) 37408–37414.
[7] C.L. Haigh, J.A. Wright, D.R. Brown, Regulation of prion protein expression by non coding regions of the Prnp gene, J. Mol. Biol. 368 (2007) 915–927.
[8] M. Scott, D. Foster, C. Mirenda, Transgenic mice expressing hamster prion protein produce species-specific scrapie infectivity and amyloid plaques, Cell 59 (1989) 847–857.
[9] K. Kashkevich, A. Humeny, U. Ziegler, M. Groschup, P. Nicken, T. Leeb, C. Fischer, C.M. Becker, K. Schiebel, Functional relevance of DNA polymorphisms within the promoter region of the prion protein gene and their association to BSE infection, FASEB J. 21 (2007) 1547–1555.
[10] N. Hunter, W. Goldmann, G. Smith, J. Hope, Frequencies of *PrP* gene variants in healthy cattle and cattle affected by BSE in Scotland, Vet. Rec. 135 (1994) 400–403.
[11] J. Lee, H.J. Lee, M.K. Shin, W.S. Ryu, Versatile PCR-mediated insertion or deletion mutagenesis, BioTechniques 36 (2004) 398–400.
[12] T. Robinson, I. Sutherland, J. Sutherland, Validation of candidate bovine references genes for use with real-time PCR, Vet. Immunol. Immunopathol. 115 (2007) 160–165.
[13] J. Yuan, A. Reed, F. Chen, C.N. Stewart, Statistical analysis of real-time PCR data, BMC Bioinformatics 7 (2006) 85–96.
[14] T. Williams, R. Tjian, Analysis of the DNA-binding and activation properties of the human transcription factor AP-2, Genes Dev. 5 (1991) 670–682.
[15] J. Yoon, G. Li, G. Roeder, Characterization of a family of related cellular transcription factors which can modulate human immunodeficiency virus type 1 transcription in vitro, Mol. Cell Biol. 14 (1994) 1776–1785.
[16] M. Oosterwegel, M. Wetering, F. Holstege, H. Prosser, M. Owen, H. Clevers, TCF-1, a T cell-specific transcription factor of the HMG box family, interacts with sequence motifs in the TCRß and TCRδ enhancers, Int. Immun. 3 (1991) 1189–1192.
[17] N. Timchenko, M. Wilde, M. Nakanishi, CCAAT/enhancer-binding protein alpha (C/EBP alpha) inhibits cell proliferation through the p21 (WAF-1/CIP-1/SDI-1) protein, Genes Dev. 10 (1996) 804–815.
[18] S. Desaint, F. Hansmannel, M. Clémencet, C. Le Jossic-Corcos, V. Nicolas-Frances, N. Latruffe, M. Cherkaoui-Malki, NFY interacts with the promoter region of two genes involved in the rat peroxisomal fatty acid β-oxidation: the multifunctional protein type 1 and the 3-ketoacyl-CoA B thiolase, Lipids Health Dis. 3 (2004) 1476–1484.
[19] A. El-Wakil, C. Francius, A. Wolff, J. Pleau-Varet, J. Nardelli, The GATA2 transcription factor negatively regulates the proliferation of neuronal progenitors, Development 133 (2006) 2155–2165.
[20] S. Culler, K. Hoff, R. Voelker, J. Berglund, C. Smolke, Functional selection and systematic analysis of intronic splicing elements identifies active sequence motifs and associated splicing factors, Nucleic Acids Res. (2010) 1–14.
[21] R. Cruz-Cosme, Y. Yamamura, Q. Tang, Roles of polypyrimidine tract binding proteins in major immediate-early gene expression and viral replication of human cytomegalovirus, J. Virol. 83 (2009) 2839–2850.
[22] C. Lemaire-Vieille, T. Schulze, V. Podevin-Dimster, J. Follet, Y. Bailly, F. Blanquet-Grossard, J. Decavel, E. Heinen, J. Cesbron, Epithelial and endothelial expression of the green fluorescent protein reporter gene under the control of bovine prion protein (PrP) gene regulatory sequences in transgenic mice, Proc. Natl. Acad. Sci. USA 97 (2000) 5422–5427.
[23] B.P. Lewis, R.E. Green, S.E. Brenner, Evidence for the widespread coupling of alternative splicing and nonsense-mediated mRNA decay in humans, Proc. Natl. Acad. Sci. USA 100 (2003) 189–192.

Cellular Immunology 263 (2010) 212–218

Contents lists available at ScienceDirect

Cellular Immunology

journal homepage: www.elsevier.com/locate/ycimm

Anti-PrP antibodies detected at terminal stage of prion-affected mouse

Yukiko Sassa [a], Natsumi Kataoka [b], Yasuo Inoshima [a], Naotaka Ishiguro [a,*]

[a] Laboratory of Food and Environmental Hygiene, Department of Veterinary Medicine, Faculty of Applied Biological Sciences, Gifu University, 1-1 Yanagido, Gifu City, Gifu 501-1193, Japan

[b] Laboratory of Veterinary Public Health, Obihiro University of Agriculture and Veterinary Medicine, Inada-cho, Obihiro, Hokkaido 080-8555, Japan

ARTICLE INFO

Article history:
Received 14 December 2009
Accepted 30 March 2010
Available online 4 April 2010

Keywords:
Anti-PrP antibody
Immune response
Prion

ABSTRACT

The causative agent of prion diseases is the pathological isoform (PrP^{Sc}) of the host-encoded cellular prion protein (PrP^{C}). PrP^{Sc} has an identical amino acid sequence to PrP^{C}; thus, it has been assumed that an immune response against PrP^{Sc} could not be found in prion-affected animals. In this study, we found the anti-prion protein (PrP) antibody at the terminal stage of mouse scrapie. Several sera from mice in the terminal stage of scrapie reacted to the recombinant mouse PrP (rMPrP) molecules and brain homogenates of mouse prion diseases. These results indicate that mouse could recognize PrP^{C} or PrP^{Sc} as antigens by the host immune system. Furthermore, immunization with rMPrP generates high titers of anti-PrP antibodies in wild-type mice. Some anti-PrP antibodies immunized with rMPrP prevent PrP^{Sc} replication *in vitro*. The mouse sera from terminal prion disease have several wide epitopes, although mouse sera immunized with rMPrP possess narrow epitopes.

1. Introduction

Prion diseases, also known as transmissible spongiform encephalopathies (TSE), are fatal neurodegenerative disorders, including scrapie in sheep and goats, bovine spongiform encephalopathy (BSE) in cattle, chronic wasting disease in deer and elk, and Creutzfeldt-Jakob disease (CJD) in humans. All of these diseases are characterized by the accumulation of a pathogenic, abnormal isoform of prion protein, designated PrP^{Sc}, in the central nervous system (CNS) [1]. PrP^{Sc} is formed from host-encoded cellular prion protein, PrP^{C}, by a post-translational process involving a profound conformational change [2].

The adaptive immune system appears unresponsive to prion infection, because the production of anti-PrP antibodies has not been recognized during the course of TSE infection, scrapie in sheep [3,4], CJD in humans [5], transmissible mink encephalopathy (TME) in mink [6], and mouse-adapted scrapie in mice [7]. The absence of a detectable immune response during TSE is likely due to the fact that the essential component of infectious agents, the prion protein (PrP), is a self-antigen expressed ubiquitously in the host. However, PrP^{Sc} may possess many unique epitopes since PrP^{Sc} has a distinct structure compared with PrP^{C}. Indeed, some monoclonal antibodies that can distinguish PrP^{Sc} from PrP^{C} [8], subtle changes in the immunoglobulin G concentrations in natural scrapie sheep [9], and T cell infiltration into the CNS in scrapie-infected mice [10] have been reported. Moreover, recent studies have reported that the humoral response against PrP can be induced not only in PrP knockout mice [11] or in xenogenic systems [12], but also in wild-type mice when tolerance to PrP was overcome by strong immunization procedures [13]. Protective immunity against scrapie agent propagation was obtained with anti-PrP antibodies when induced by active immunization [14,15] or injected passively [16]. Thus, the host immune system may produce antibodies against PrP^{Sc} and interfere with the progression of prion diseases; however, little is known about the immune response to PrP^{Sc} in prion-infected animals.

We recently found several antibody titers against the recombinant mouse PrP (rMPrP) at the terminal stage of scrapie infection in mouse. In this study, we investigated the characteristics of the antibody titers at the terminal stage and their protective effect against scrapie infection in the mouse model.

2. Materials and methods

2.1. Animals

Four- to six-week-old female C57BL/6J, BALB/c, ICR, NOD and A/J mice supplied by CLEA (Tokyo, Japan) were kept in a specific pathogen-free animal facility. The animal experiments were performed according to the Regulations for Animal Experiments of Gifu University and were approved by the committee for Animal Research and Welfare at Gifu University.

2.2. Purification of PrP^{Sc}

PrP^{Sc} was purified from the brains of scrapie-affected mice without proteinase K treatment as described by Bolton et al. [17].

* Corresponding author. Fax: +81 58 293 2864.
E-mail address: ishiguna@gifu-u.ac.jp (N. Ishiguro).

0008-8749/$ - see front matter © 2010 Elsevier Inc. All rights reserved.
doi:10.1016/j.cellimm.2010.03.018

The brains of C57BL/6J, BALB/c and ICR mice inoculated intracerebrally with mouse-adapted scrapie Obihiro strain [18] were used as the source of PrP^{Sc}.

2.3. Sera from mice inoculated with prion for screening

Inoculation of mice with prion was performed according to Table 1. Mice sera were collected at the terminal stage of the disease under anesthesia. The obtained sera were stored at −30 °C.

2.4. Synthesis of rMPrP

The rMPrP corresponding to amino acid (aa) 23–231 was synthesized in *Escherichia coli* BL21 (DE3), purified by Ni^{2+} immobilized metal affinity chromatography as described by Kim et al. [19]. The purified rMPrP was dissolved in distilled deionized water (DDW) at 1 mg/ml and stored at −80 °C.

2.5. Immunizations and bioassay of mice

Twenty mice were immunized intraperitoneally with 50 μl of rMPrP (1 mg/ml in DDW) emulsified with complete Freund's adjuvant (CFA) in a 1:1 (v/v) ratio. Two weeks after the first immunization, animals were boosted with an equivalent rMPrP emulsion prepared with incomplete Freund's adjuvant (IFA). Nine weeks after immunization, 100 μl of 0.01% mouse scrapie brain homogenate was injected intraperitoneally, and survival periods were observed. Animals immunized with phosphate-buffered saline (PBS) instead of rMPrP were used as a negative control ($n = 4$). Immunized mice were bled from retro-orbital plexus at the time of pre-immunization ($n = 20$), at 8 weeks ($n = 20$), at 16 weeks ($n = 8$) and at 43 weeks ($n = 16$) after immunization. Individuals who showed higher antibody titers at 8 weeks were selected for bleeding at 16 weeks and at the terminal stage of the disease ($n = 14$: Serum Nos. a–h). The obtained sera were stored at −30 °C.

2.6. Enzyme-linked immunoabsorbent assay (ELISA)

Ninety-six-well plates (MaxiSorp, Nunc, Roskild, Denmark) were coated overnight at 4 °C with 0.2 μg/well, rMPrP or purified PrP^{Sc} in 20 mM phosphate buffer (pH 7.0) or 1% brain homogenate. Brain homogenates of BALB/c mice infected with mouse scrapie Obihiro strain or those of ICR mice infected with mouse-adapted BSE strain were denatured with 3 M guanidine hydrochloride (Gdn-HCl). The wells were blocked with 5% skim milk in PBS containing 0.1% Tween 20 (PBST) for 1 h at 37 °C, and then incubated with sera diluted to 1:100 in 1% skim milk/PBST for 1 h at 37 °C. After washing with PBST, wells were incubated with anti-mouse IgG horse radish peroxides (HRP)-conjugated antibody for 1 h. Antigen–antibody complexes were detected by adding a substrate solution [100 μg/ml of 2,2′-azino-bis(3-ethylbenzthiazoline-6-sulfonic acid), 0.04% H_2O_2 in 50 mM citrate-phosphate buffer (pH 4.0)] and an absorbance at 405 nm was assessed with a microplate reader (Multiscan MS-UV, Labsystems, Uppsala, Sweden).

2.7. Cell culture

The mouse neuroblastoma cell line Neuro2a-3 (N2a-3) cells, a highly PrP^{Sc} susceptible clone of N2a cells for mouse-adapted scrapie, was cultured in Dulbecco's modified Eagle's medium (DMEM) with 10% fetal bovine serum, 100 U/ml of penicillin, 100 mg/ml of streptomycin and non-essential amino acids. ScN2a-3 cells were established from N2a-3 cells exposed to 0.5% Chandler-affected mouse brain homogenate diluted in growth medium for 4 h at 37 °C in 5% CO_2. Cells were washed with PBS and cultured with fresh growth medium. ScN2a-3 cells were used for assay from 5 to 10 passages that showed high level of scrapie infectivity titers (data not shown). These cells were maintained at 37 °C in 5% CO_2 and passed at 1:10 every 3 days.

2.8. Treatment of ScN2a-3 and sample preparation

Almost-confluent ScN2a-3 cells in 25-cm^2 flasks were split 1:20 into 35-mm tissue culture dishes. On day 2, the medium was replaced with 3 ml DMEM containing 4% FBS, and each test serum (1:100) or monoclonal antibody (mAb) 31C6 [19] (1:2000) was added, and the cells were then cultured for 3 additional days. For the detection of PrP^{Sc}, cells were lysed with 300 μl lysis buffer (5 mM EDTA, 0.5% Triton X-100, 0.5% sodium deoxycholate, 150 mM NaCl, and 10 mM Tris–HCl, pH 7.5) and kept at 4 °C for 30 min. Cell debris was removed by centrifugation for 5 min at 1300 rpm. A portion of the sample (10%) was removed for determination of protein concentration using the DC protein assay (BioRad, Hercules, CA, USA) and the remaining portions were treated with 20 μg/ml proteinase K for 20 min at 37 °C. Proteolysis was terminated by the addition of 1 mM Pefabloc (Roche, Indianapolis, IN, USA). The samples were then incubated with 0.3% sodium phosphotungstic acid at 37 °C for 30 min. The samples were centrifuged at 15,500g for 30 min, and the resulting pellets were dissolved in sample buffer (62.5 mM Tris–HCl (pH 6.8), 5% glycerol, 3 mM EDTA, 5% SDS, 4 M urea, 4% 2-ME, 0.04% bromophenol blue).

2.9. Western blotting

Samples were separated in 12% SDS–PAGE, and electrotransferred to Immobilon-P membranes (Millipore, Bedford, MA, USA). The membranes were blocked with 5% skim milk/PBST, and incubated with mAb 44B1 [19] diluted to 1:5000 in 1% skim milk/PBST for 1 h. After incubation with HRP-conjugated secondary antibody, the blots were developed using ECL™ Western blotting detection reagents (GE Healthcare, Buckinghamshire, UK), and the signals were detected with a LAS-4000 luminoimage analyzer (Fujifilm, Tokyo, Japan).

2.10. Pepspot analysis

Pepspot membrane, consisting of 100 peptides of 10 amino acids in length with two amino acids overlapping to adjacent peptides and encompassing full-length mature murine PrP (PrP 23–231), was synthesized by SIGMA-Genosys. The membrane was blocked with 5% skim milk and 5% sucrose in Tris-buffered saline containing 0.05% Tween 20 (TBST), and incubated with sera (dilute at 1:100). Bound antibodies were detected by using the HRP-conjugated secondary antibodies and an ECL™ Western blotting detection reagents, and the signals were detected with X-ray films (Fujifilm).

2.11. Statistical analyses

The data were analyzed statistically by parametric correlation analyses using the software package ystat2006 programmed by Shinya Yamazaki, DDS, PhD (Igaku Tosho Shuppan Co., Ltd., Tokyo, Japan).

3. Results

3.1. Detection of anti-PrP antibodies in terminal stage of scrapie

To estimate the production of antibodies to PrP, 143 sera from prion-affected C57BL/6J, BALB/c, ICR, NOD and A/J mice were screened by ELISA using rMPrP as antigens (Table 1A). Eight of 143

sera reacted with rMPrP (OD values; 0.108 ± 0.015–0.314 ± 0.015). However, we could not detect any signals when using the purified PrP^{Sc} fraction as an ELISA antigen (Table 1A).

Furthermore, 117 sera obtained from prion-affected C57BL/6J, BALB/c and ICR mice were screened by ELISA using three antigens: rMPrP, mouse brain homogenate of mouse scrapie Obihiro strain and mouse brain homogenate of mouse-adapted BSE strain. Seven sera were positive for rMPrP (OD values; 0.079 ± 0.005–0.365 ± 0.066), eight sera were positive for mouse brain homogenate of Obihiro strain (OD values; 0.061 ± 0.011–0.233 ± 0.013), and six sera were positive for mouse brain homogenate of mouse-adapted BSE strain (OD values; 0.070 ± 0.004–0.213 ± 0.005) (Tables 1B and 2). Although the OD titers were low, the positive sera showed higher absorbance than the cut-off value for at least three independent assays. Six sera bound to two of the three tested antigens (Table 2). Fifteen of 117 sera showed anti-PrP antibody titers against at least one antigen. Some sera with anti-PrP antibodies were subjected to Western blot analyses using PK treated Obihiro brain homogenates as an antigen, however, any sera could not detect PrP^{Sc}. The immune response against PrP has not been supposed to be occurred because the host has the endogenous PrP ubiquitously. However, we showed the anti-PrP antibodies in prion-affected mice. Therefore, to confirm the production of anti-PrP antibody in wild-type mice, we immunized mice with rMPrP using conventional immunization method.

3.2. Immunization generates high levels of antibodies to rMPrP, but does not possess prophylactic effect against disease

To confirm a PrP-specific immune response, we intraperitoneally immunized BALB/c mice with rMPrP twice at 2-week intervals.

Table 1
Detection of anti-PrP antibodies in terminal-stage mouse prion disease.

Mouse strain	Inoculum[a]	Injection route[b]	Mice with antibodies against PrP			
			rMPrP	Purified PrP^{Sc}	Obihiro[a]	Mouse-adapt BSE[a]
C57BL/6J	1% Obihiro	i.c.	0/43	0/43	ND[c]	ND
	Purified PrP^{Sc}	i.p.	0/5	0/5	ND	ND
BALB/c	1% Obihiro	i.c.	2/40	0/40	ND	ND
	Purified PrP^{Sc}	i.p.	0/5	0/5	ND	ND
	10% Obihiro	i.p.	0/5	0/5	ND	ND
	Purified PrP^{Sc}	Footpad	0/4	0/4	ND	ND
ICR	1% Obihiro	i.c.	6/33	0/33	ND	ND
	10% Obihiro	s.c.	0/3	0/3	ND	ND
NOD	Purified PrP^{Sc}	i.p.	0/2	0/2	ND	ND
A/J	Purified PrP^{Sc}	i.p.	0/3	0/3	ND	ND
C57BL/6J	0.05% Obihiro	i.p.	0/17	ND	0/17	0/17
BALB/c	0.01% Obihiro	i.p.	0/4	ND	0/4	0/4
	1% Obihiro	i.p.	7/70	ND	3/70	0/70
ICR	1% mouse-adapt BSE	i.c.	0/13	ND	4/13	4/13
	1% Chandler	i.c.	0/13	ND	1/13	2/13

[a] Purified PrP^{Sc} was prepared from brains of Obihiro-affected mice. Brain homogenates are indicated for Obihiro, Mouse-adapt BSE, and Chandler.
[b] i.c., intracerebrally; i.p., intraperitoneally; s.c., subcutaneously.
[c] ND, not done.

Table 2
Positive PrP response in ELISA.

Mouse strain	Inoculum[a]	Injection route[b]	ID	OD titers against PrP[c]		
				rMPrP	Obihiro	Mouse-adopt BSE
BALB/c	1% Obihiro	i.p.	1	0.147 ± 0.022	–	–
			2	0.124 ± 0.003	–	–
			3	0.253 ± 0.008	0.150 ± 0.024	–
			4	0.365 ± 0.066	0.233 ± 0.013	–
			5	0.081 ± 0.018	–	–
			6	0.079 ± 0.005	–	–
			7	0.097 ± 0.006	–	–
			8	–	0.072 ± 0.012	–
ICR	1% mouse-adapt BSE	i.c.	9	–	0.080 ± 0.028	0.070 ± 0.004
			10	–	0.142 ± 0.025	0.163 ± 0.007
			11	–	–	0.077 ± 0.004
			12	–	0.172 ± 0.008	0.213 ± 0.005
			13	–	0.061 ± 0.011	–
	1% Chandler	i.c.	14	–	–	0.135 ± 0.005
			15	–	0.062 ± 0.003	0.088 ± 0.009
Negative control[d]				0.019 ± 0.001	0.015 ± 0.006	0.034 ± 0.008
Cut-off value[e]				0.022	0.032	0.056

[a] Brain homogenates are indicated for Obihiro, mouse-adapt BSE, and Chandler.
[b] i.c., intracerebrally; i.p., intraperitoneally.
[c] Serum were diluted 1:100, and OD titers are shown as mean ± SD. "–" means that OD titers against PrP was less than cut-off value.
[d] Normal mouse serum was used for negative control.
[e] Cut-off values were calculated by the AVG+ 3SD of negative control.